Bidentate chelate complexes of palladium(II) with the carbanion 2-C 6F4PPh2 and their transformation into complexes containing bridging 2-C6F4PPh2

ARTICLE *in* ORGANOMETALLICS · JANUARY 2011

Impact Factor: 4.13

8 AUTHORS, INCLUDING:

Alan David Rae

Australian National University

242 PUBLICATIONS **4,137** CITATIONS

SEE PROFILE

Suresh Bhargava

RMIT University

431 PUBLICATIONS **3,700** CITATIONS

SEE PROFILE

ORGANOMETALLICS

ARTICLE

pubs.acs.org/Organometallics

Bidentate Chelate Complexes of Palladium(II) with the Carbanion 2-$C_6F_4PPh_2$ and Their Transformation into Complexes Containing Bridging 2-$C_6F_4PPh_2$

Martin A. Bennett,[†] Gopa Kar,[‡] Nedaossadat Mirzadeh,[‡] Steven H. Privér,[‡] A. David Rae,[†] Jörg Wagler,[§] Anthony C. Willis,[†] and Suresh K. Bhargava*[,‡]

[†]Research School of Chemistry, Australian National University, Canberra, ACT 0200, Australia

[‡]School of Applied Sciences (Applied Chemistry), RMIT University, GPO Box 2476 V, Melbourne, Victoria 3001, Australia

[§]Institut für Anorganische Chemie, Technische Universität Bergakademie, Freiberg D-09596, Germany

ABSTRACT: Reaction of the organotin compound 2-$Me_3SnC_6F_4PPh_2$ (**7**) with the cycloocta-1,5-diene complexes [PdX_2(cod)] at room temperature gives dinuclear halide-bridged palladium(II) complexes [$Pd_2(\mu\text{-X})_2(\kappa^2\text{-2-}C_6F_4PPh_2)_2$] [X = Cl (**5**), Br (**8**)] in which the carbanions are present as four-membered chelate rings. The bridging halides can be replaced by various anions, giving the corresponding dinuclear complexes having X = O_2CCH_3 (**9**), O_2CPh (**10**), I (**12**), and SCN (**15**), and by acetylacetonate anion (acac) to give mononuclear [Pd(acac)-(κ^2-2-$C_6F_4PPh_2$)] (**17**). In solution at room temperature the four-membered κ^2-2-$C_6F_4PPh_2$ rings open, probably by one-ended dissociation of a Pd−P bond, to give compounds of the same composition containing bridging 2-$C_6F_4PPh_2$ units, e.g., [$Pd_4(\mu\text{-X})_4(\mu$-2-$C_6F_4PPh_2)_4$] [X = Cl (**6**), I (**13**)], [$Pd_2(\mu\text{-}O_2CCH_3)_2(\mu$-2-$C_6F_4PPh_2)_2$] (**11**), and [$Pd_2$(acac)$_2(\mu$-2-$C_6F_4PPh_2)_2$] (**18**). In some cases, only half the available chelate rings open; for example, complex **15** gives [$Pd_4(\mu\text{-SCN})_4(\mu$-2-$C_6F_4PPh_2)_2(\kappa^2$-2-$C_6F_4PPh_2)_2$] (**16**) and complex **12** gives [$(\kappa^2$-2-$C_6F_4PPh_2)$Pd(μ-I)(μ-2-$C_6F_4PPh_2$)Pd(μ-I)$_2$Pd(μ-I)(μ-2-$C_6F_4PPh_2$)Pd(κ^2-2-$C_6F_4PPh_2$)] (**14**), in addition to **13**. Ring-opening also occurs on addition of acetonitrile to **5** or **8**, forming [$Pd_2X_2(NCMe)_2(\mu$-2-$C_6F_4PPh_2)_2$] [X = Cl (**19**), Br (**20**)]. Treatment of **8** with two equivalents of PPh_3 forms [PdBr(κ^2-2-$C_6F_4PPh_2$)(PPh_3)] (**21**) as a *cis*−*trans* mixture, which reacts with more PPh_3 to give *trans*-[PdBr(κC-2-$C_6F_4PPh_2$)($PPh_3)_2$] (**23**) by displacement of the Pd−P bond of the chelate ring. The bulkier ligand tricyclohexylphosphine reacts with **8** to give an analogue (**22**) of **21**, but it does not open the chelate ring. The X-ray structures of compounds **7**−**11**, **13**−**21**, and **23** are reported.

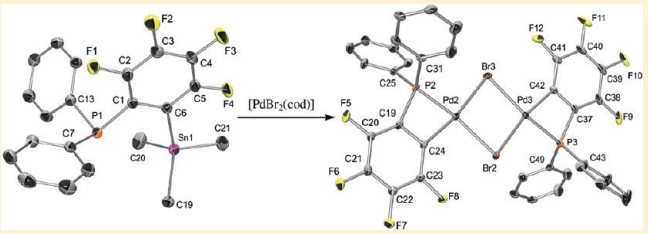

INTRODUCTION

Since the discovery of the *ortho*-palladation of azobenzene and *N*,*N*-dimethylaniline in the 1960s,[1,2] cyclopalladated complexes, especially those containing N-, O-, and S-donor groups, have attracted continuous interest because of their diverse applications, particularly in organic synthesis, and because of the relevance of cyclopalladation to the transition metal promoted C−H activation of hydrocarbons.[3−16] Cyclopalladation of P-donor groups by C−H activation[6,9,11−17] is generally observed only with very bulky or sterically constrained tertiary phosphines or with phosphites; *ortho*-palladated complexes of triphenylphosphine cannot be obtained by this route. Attempts to make them from Pd(0) or Pd(II) precursors by transmetalation from [Hg(2-$C_6H_4PPh_2)_2$] gave exclusively complexes in which 2-$C_6H_4PPh_2$ bridges Pd and Hg.[17,18] However, Lahuerta et al.[19,20] have shown that 2-$BrC_6H_4PPh_2$ adds oxidatively to the palladium(0)-dibenzylideneacetone complex, [Pd(dba)$_2$], to give a tetranuclear complex [$Pd_4(\mu\text{-Br})_4(\mu$-2-$C_6H_4PPh_2)_4$] (**1**), in which an approximate rectangle of palladium atoms is bridged on alternate sides either by two bromine atoms or by two 2-$C_6H_4PPh_2$ units arranged head-to-tail. The tetramer array is broken down to binuclear fragments **2** and **3** on treatment with silver acetate or trifluoroacetate and with PMe_3 or PMe_2Ph, respectively, the bridging 2-$C_6H_4PPh_2$ groups being retained. Bulkier tertiary phosphines, such as PPh_3 or PCy_3, give monomeric species [PdBr(κ^2-2-$C_6H_4PPh_2$)(L)] (L = PPh_3, PCy_3) containing a four-membered P−C chelate ring. This chemistry is summarized in Scheme 1. Related examples of the interconversion between the bridging and chelate coordination modes of 2-$C_6H_4PPh_2$ and its congeners have also been observed in platinum and gold chemistry.[21−23]

The stability of complexes containing four-membered chelate rings is increased if the *o*-phenylene hydrogen atoms of 2-$C_6H_4PPh_2$ are replaced by fluorine. The bis(chelate) palladium(II) complex *trans*-[$Pd(\kappa^2\text{-}P,C$-2-$C_6F_4PPh_2)_2$], the 2-$C_6H_4PPh_2$ analogue of which is unknown, undergoes ligand scrambling with [$PdCl_2$-(NCMe)$_2$] to give the binuclear species [$Pd_2(\mu\text{-Cl})_2(\kappa^2\text{-}P,C$-2-$C_6F_4PPh_2)_2$] (**5**), shown in Scheme 2;[24] **5** rearranges slowly in

Received: February 24, 2011
Published: June 22, 2011

Scheme 1

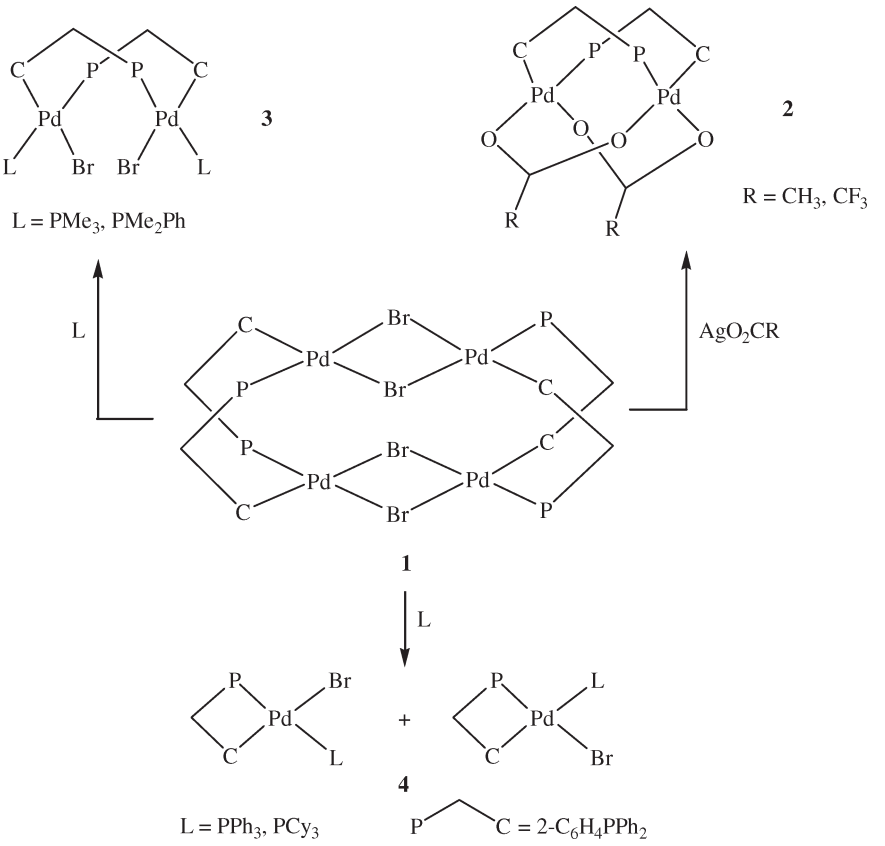

Scheme 2

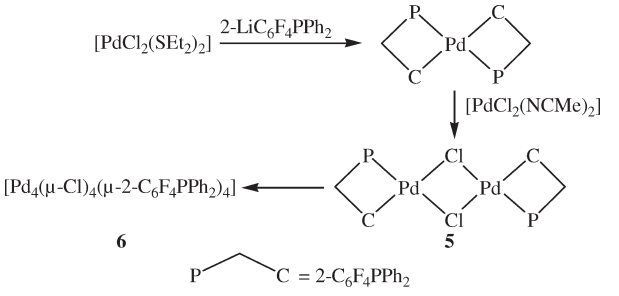

solution by opening of the chelate rings to a tetranuclear complex of the same composition as **5**, $[Pd_4(\mu\text{-}Cl)_4(\mu\text{-}2\text{-}C_6F_4PPh_2)_4]$ (**6**), which is structurally analogous to **1**. We now report the behavior of the corresponding bromide, iodide, carboxylate, pseudohalide, and acetylacetonato derivatives, thereby establishing the existence of a family of *ortho*-palladated compounds of a similar type, i.e., of identical composition but containing either chelate κ^2-*P*,*C*-2-$C_6F_4PPh_2$ or bridging μ^2-*P*,*C*-2-$C_6F_4PPh_2$. We have also discovered two compounds that display both coordination modes. Finally, we report reactions of **5** and **8** with acetonitrile and of **8** with PPh_3 and PCy_3, which also lead to irreversible opening of the chelate ring.

RESULTS AND DISCUSSION

Transmetalation from the organotin compound 2-$Me_3SnC_6F_4PPh_2$ (**7**) provided a convenient route to the palladium(II) complexes required for this study. This precursor was obtained in ca. 85% yield as a colorless, air-stable solid by treating an ether solution of 2-$BrC_6F_4PPh_2$, cooled to −78 °C, sequentially with ^{n}BuLi and Me_3SnCl. Its ESI-mass spectrum showed a $[M + H]^+$ peak at m/z 499, and the ^{1}H NMR spectrum contained, in addition to the expected aromatic multiplets, a triplet resonance at δ 0.48

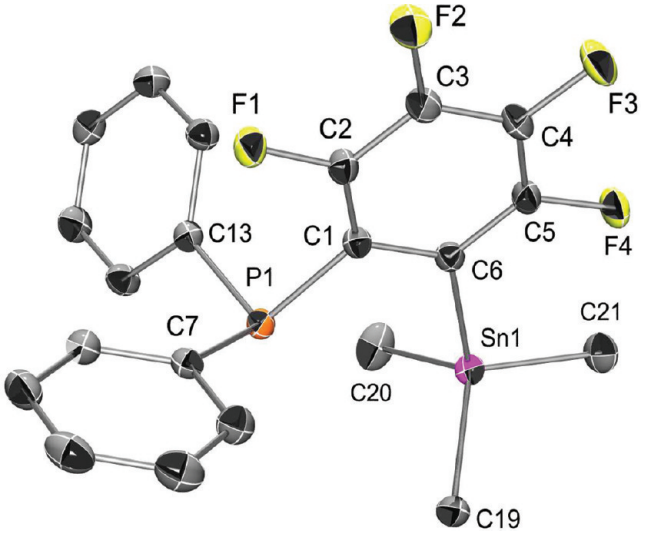

Figure 1. Molecular structure of 2-$Me_3SnC_6F_4PPh_2$ (**7**). Ellipsoids show 50% probability levels, and hydrogen atoms have been omitted for clarity. Only one molecule of the asymmetric unit is shown.

dx.doi.org/10.1021/om200179v |*Organometallics* 2011, 30, 3749–3762

Scheme 3

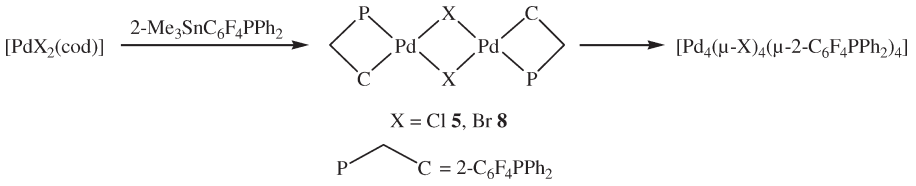

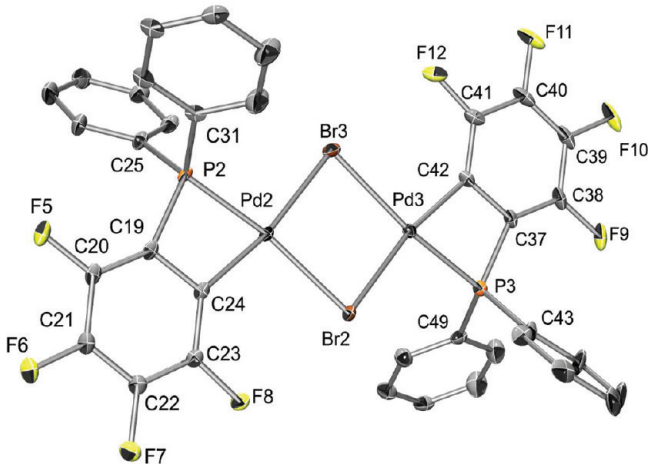

Figure 2. Molecular structure of $[Pd_2(\mu\text{-}Br)_2(\kappa^2\text{-}2\text{-}C_6F_4PPh_2)_2]$ (**8**), one of the 4.5 independent molecules in the asymmetric unit (see Experimental Section). Ellipsoids show 30% probability levels, and hydrogen atoms and a dichloromethane molecule have been omitted for clarity. Selected bond distances (Å) and angles (deg): Pd(2)−Br(2) 2.510(2), Pd(2)−Br(3) 2.524(2), Pd(3)−Br(3) 2.517(2), Pd(3)−Br(2) 2.518(2), Pd(2)−P(2) 2.214(3), Pd(3)−P(3) 2.216(4), Pd(2)−C(24) 2.013(4), Pd(3)−C(42) 2.011(4), P(3)−Pd(3)−C(42) 69.03(2), Pd(2)−Br(3)−Pd(3) 91.2(1), Pd(2)−Br(3)−Pd(3) 91.2(1), Pd(2)−Br(2)−Pd(3) 91.8(1), Br(2)−Pd(3)−Br(3) 88.3(1), Br(3)−Pd(2)−Br(2) 88.6(1), P(2)−Pd(2)−C(24) 69.5(2).

(J = 1.6 Hz) due to the $SnMe_3$ group together with $^{117/119}Sn$ satellites (J = 54.9, 57.8 Hz). In the ^{13}C NMR spectrum, the $SnMe_3$ resonance at δ −3.9 was split into a doublet of doublets (J = 4.5, 13.3 Hz), presumably arising from three-bond coupling to the *ortho* fluorine and phosphorus atoms on the aromatic ring. Equally spaced about the main resonance were satellites arising from the ^{117}Sn and ^{119}Sn isotopomers (J = 361 and 381 Hz). The ^{31}P NMR spectrum showed a doublet of multiplets centered at δ −0.2 with poorly resolved $^{117/119}Sn$ coupling of ca. 29 Hz. The X-ray structure of **7** is shown in Figure 1; the C(methyl) bond lengths [2.138(2)−2.148(2) Å] are comparable to those found in $(CH_3)_4Sn$ [2.144(3) Å].[25] In contrast, the Sn−C(aryl) bond length [2.1883(14) and 2.1904(15) Å for two independent molecules] is significantly greater than the corresponding distances in $(C_6H_5)_4Sn$ [2.137(5) Å][26] and $(C_6F_5)_4Sn$ [2.126(8) Å],[27] presumably owing to the presence of the bulky *ortho*-PPh_2 substituent. Because of the less Lewis acidic Sn site (devoid of Sn-bound halide), the P···Sn separation in **7** [3.3694(4) and 3.3931(4) Å] is greater than those reported in $[o\text{-}Ph_2PC_6H_4(SnPh_2Cl)]$ [3.125(4) Å] and $[(o\text{-}^iPr_2PC_6H_4)_2SnPhCl]$ [3.120(1) Å].[28]

Reaction of equimolar quantities of $2\text{-}Me_3SnC_6F_4PPh_2$ (**7**) and $[PdX_2(cod)]$ (X = Cl, Br) over a period of 2 h at room temperature gave dimeric palladium complexes $[Pd_2(\mu\text{-}X)_2(\kappa^2\text{-}2\text{-}C_6F_4PPh_2)_2]$ [X = Cl (**5**), Br (**8**)] as yellow or orange, air-stable solids in high yields (Scheme 3). Using a 2.5:1 molar ratio of **7** to $[PdX_2(cod)]$, **5** or **8**, in refluxing CH_2Cl_2 for 24 h gave the previously reported bis(chelate) complex *trans*-$[Pd(\kappa^2\text{-}2\text{-}C_6F_4PPh_2)_2]$.[24]

A single-crystal X-ray structural determination showed that complex **8** consists of two palladium atoms bridged by a pair of bromine atoms and coordinated to two chelate $2\text{-}C_6F_4PPh_2$ ligands, the phosphorus and carbon atoms of the latter being, separately, mutually *trans* across the planar Pd_2Br_2 unit. The molecular structure is shown in Figure 2 together with selected bond lengths and angles.

The metal atoms display the expected planar coordination, distorted as a consequence of the narrow bite angle (69°) of the $\kappa^2\text{-}C_6F_4PPh_2$ ligands, this value being typical of this mode of coordination.[29] The Pd−Br−Pd bridges are almost symmetrical, and the Pd−Br bond lengths [2.517 Å (av)] are close to those found in the tetranuclear complex **1** [2.510 Å (av)];[19] the Pd−P and Pd−C bond lengths in the two compounds are also similar.

The ESI-mass spectra of **5** and **8** each showed peaks corresponding to the $[M + Na]^+$ ions. The ^{31}P NMR spectra of each compound showed a pair of resonances at about δ −76 and −77, indicating the presence in solution of two species containing a phosphorus atom in a four-membered chelate ring.[31] The relative intensities of the two peaks varied in different preparations, the less shielded resonance always being the more intense. The less intense resonance may correspond to the *cis* isomer of $[Pd_2(\mu\text{-}X)_2(\mu\text{-}2\text{-}C_6F_4PPh_2)_2]$. In potentially coordinating solvents such as acetone and THF, only one resonance was observed, probably because of reversible cleavage of the Pd_2Br_2 bridges.

Over a period of weeks at room temperature the ^{31}P NMR high-field resonances in CH_2Cl_2 solutions of **5** and **8**, characteristic of the four-membered P−C chelates, decreased in intensity and a new peak at δ ca. 28 assignable to the tetranuclear complexes $[Pd_4(\mu\text{-}X)_4(\mu\text{-}2\text{-}C_6F_4PPh_2)_4]$ (X = Cl, Br) was observed. As already reported,[24] the tetranuclear chloro complex could be isolated in ca. 40% yield from the resulting solution, but the reaction in the case of X = Br was accompanied by considerable decomposition and the appearance of several additional, unassigned ^{31}P NMR signals. However, the tetranuclear bromo complex was formed in high yields in CH_2Cl_2/MeOH over 5 d at room temperature. Lahuerta et al.[30] have isolated this compound in moderate yield from the oxidative addition of $2\text{-}BrC_6F_4PPh_2$ to $[Pd(dba)_2]$, although a tedious purification procedure was required. The tetranuclear chloro complex was formed in slightly higher yields (ca. 50%) in CH_2Cl_2/MeOH.

We now turn to the reactions of **8** with various ligands.

a. Carboxylate Ions (Scheme 4). Reaction of complex **8** with a small excess of silver acetate or benzoate in CH_2Cl_2 gave the corresponding carboxylate complexes $[Pd_2(\mu\text{-}O_2CR)_2$

Scheme 4

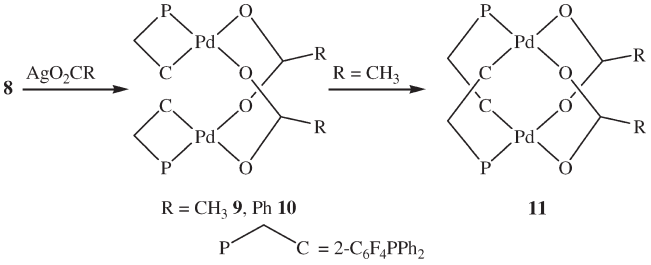

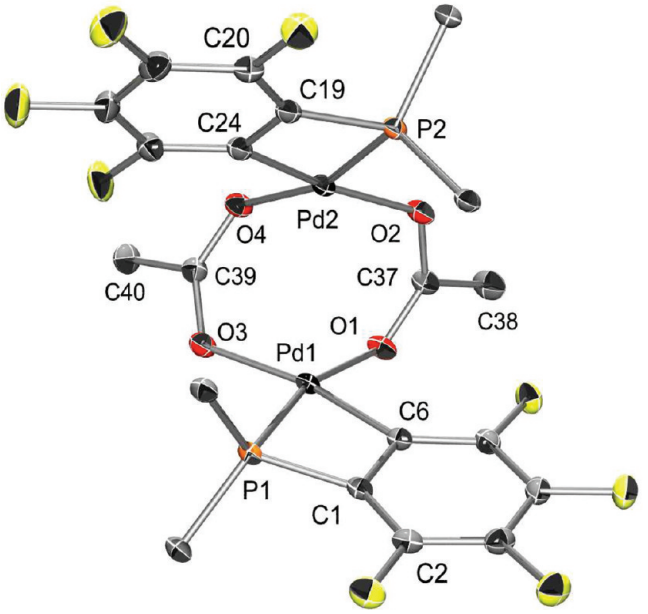

Figure 3. Molecular structure of $[Pd_2(\mu\text{-}O_2CCH_3)_2(\kappa^2\text{-}2\text{-}C_6F_4PPh_2)_2]$ (**9**). Ellipsoids show 50% probability levels. Hydrogen atoms have been omitted for clarity, and only the *ipso* carbons of the PPh_2 groups are shown. The structure contains 0.5 C_6H_6 (not shown) in the asymmetric unit. Selected bond distances (Å) and angles (deg): Pd(1)···Pd(2) 2.9897(2), Pd(1)−P(1) 2.2318(3), Pd(2)−P(2) 2.2294(3), Pd(1)−C(6) 1.9886(13), Pd(2)−C(24) 1.9951(14), Pd(1)−O(1) 2.0988(9), Pd(1)−O(3) 2.0951(10), Pd(2)−O(2) 2.0930(10), Pd(2)−O(4) 2.1043(9), P(1)−Pd(1)−C(6) 69.93(4), C(24)−Pd(2)−P(2) 69.92(4). Corresponding data for **10**: Pd(1)···Pd(2) 2.9627(2), Pd(1)−P(1) 2.2247(4), Pd(2)−P(2) 2.2115(4), Pd(1)−C(6) 1.9901(14), Pd(2)−C(24) 1.9886(14), Pd(1)−O(1) 2.0886(10), Pd(1)−O(3) 2.0938(11), Pd(2)−O(2) 2.0836(11), Pd(2)−O(4) 2.0981(10), P(1)−Pd(1)−C(6) 69.76(4), C(24)−Pd(2)−P(2) 69.83(4).

$(\kappa^2\text{-}2\text{-}C_6F_4PPh_2)_2]$ [R = CH_3 (**9**), Ph (**10**)] in good yields as pale yellow solids. Each showed in its ^{31}P NMR spectrum in C_6D_6 a single broad resonance at δ ca. −74, confirming that the chelate 2-$C_6F_4PPh_2$ group was still present, and the ^1H NMR spectrum of **9** contained a singlet at δ 2.26 arising from the acetate methyl group. The IR spectrum of **9** exhibited two strong bands at 1421 and 1567 cm^{-1} assignable to symmetric and asymmetric COO vibrations, the separation being indicative of bridging acetate groups.[32] There was no evidence for the formation of mononuclear species containing chelating 2-$C_6F_4PPh_2$ and carboxylate groups.

The molecular structures of **9** and **10** have been determined by X-ray crystallography; that of **9** is shown in Figure 3, together with selected bond lengths and angles. The structures resemble that of **8** in possessing a pair of palladium atoms that are coordinated to chelate 2-$C_6F_4PPh_2$ ligands and bridged by two carboxylate groups; however, in contrast to **8**, the chelate rings do not lie along the Pd−Pd axis but are stacked orthogonally to it. Consequently the Pd−Pd separations in **9** and **10** [2.9897(2), 2.9627(2) Å, respectively] are considerably less than that in **8** [3.596(2), 3.603(2), 3.611(2), 3.619(2), 3.639(2) Å for 4.5 independent molecules]. Similar structures are observed for μ-carboxylato *o*-palladated N-donor complexes, such as $[Pd_2(\mu\text{-}OAc)_2(\kappa^2\text{-}C,N\text{-}2\text{-}C_6H_4C_5H_4N)_2]$[33] and $[Pd_2(\mu\text{-}OAc)_2(\kappa^2\text{-}C,N\text{-}C_{13}H_8N)_2]$[34] derived from 2-phenylpyridine and benzoquinoline, respectively. It has been argued, on the basis of the observed Pd···Pd separations (ca. 2.85 Å), the photophysical properties of the complexes, and computational analysis, that there is an attractive interaction between the $4d^8$ metal centers.[33] Any such interaction is likely to be weaker in complexes **9** and **10**. The bite angles of the chelate 2-$C_6F_4PPh_2$ groups in **9** and **10** are about 69°, as expected. The Pd−O bond lengths *trans* to phosphorus are close to those *trans* to σ-carbon atoms (ca. 2.10 Å), indicative of a similar *trans* influence for these ligands.

When a solution of **9** in toluene/methanol was set aside at room temperature, the intensity of the high-field signal in the ^{31}P NMR spectrum (δ −75.4 in this medium) diminished and a peak at δ 15.6 began to appear. After 4 d, the latter was more intense, but only after several weeks had the high-field signal disappeared and the peak at δ 15.6 was now accompanied by several additional resonances of unknown origin, including an intense peak at δ 53.3. The peak at δ 15.6 is assigned to the isomeric compound $[Pd_2(\mu\text{-}O_2CCH_3)_2(\mu\text{-}2\text{-}C_6F_4PPh_2)_2]$ (**11**) [δ_P ($CDCl_3$) 15.5], which has been isolated by Lahuerta et al.[30] from the reaction of $[Pd_4(\mu\text{-}Br)_4(\mu\text{-}2\text{-}C_6F_4PPh_2)_4]$ with silver acetate. Although we could not convert the κ^2- into a μ-2-$C_6F_4PPh_2$ acetato complex quantitatively, X-ray structure analyses of two single crystals grown from a partly isomerized solution of **9** confirmed the assignment. One of the single crystals was unsolvated but crystallized in the orthorhombic space group $Pna2_1$, in contrast to the monoclinic space group $C2/c$ reported by Lahuerta and co-workers.[30] The second crystal was in the latter space group, the cell dimensions being similar (though not identical) to those reported by Lahuerta and co-workers,[30] and contained 1 mol of C_6H_6 per formula unit. The relatively high *R*-factor of the structure reported by Lahuerta et al. (8.56% for the observed reflections) may arise from unrefined solvent that is disordered
in a diffuse fashion within the voids provided by the crystal lattice. However, the molecular dimensions of the dinuclear palladium complex in the three forms do not differ significantly. The Pd···Pd separations in our two forms [2.68969(4), 2.68159(15) Å, respectively] are ca. 0.3 Å less than in complexes **9** and **10**, indicative of a stronger metal−metal interaction induced by the two additional bridging groups; these values fall in the range 2.55−2.74 Å observed in binuclear Pd(II) complexes containing four bridging ligands with N−N, N−O, N−S, and S−S donor sets.[35]

b. Iodide Ions (Scheme 5). Treatment of the acetato complex **9** with an excess of sodium iodide in methanol gave $[Pd_2(\mu\text{-}I)_2(\kappa^2\text{-}2\text{-}C_6F_4PPh_2)_2]$ (**12**) as a brown solid that proved difficult to isolate reproducibly in a pure state. It was also formed from **8** and NaI, but, in this case also, other unidentified products

Scheme 5

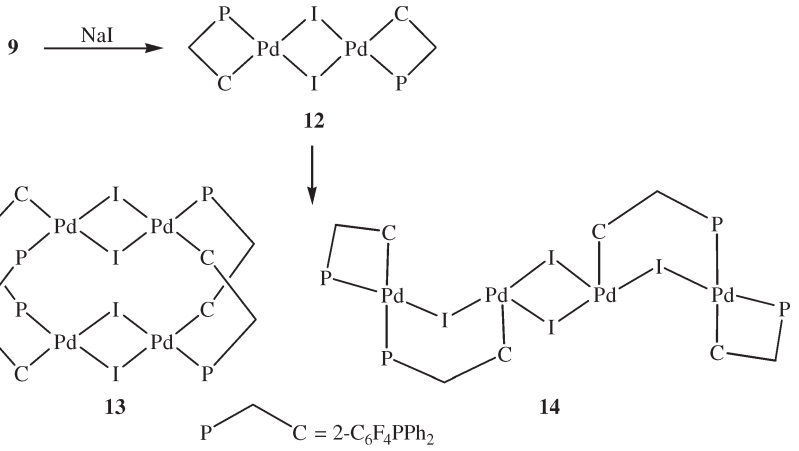

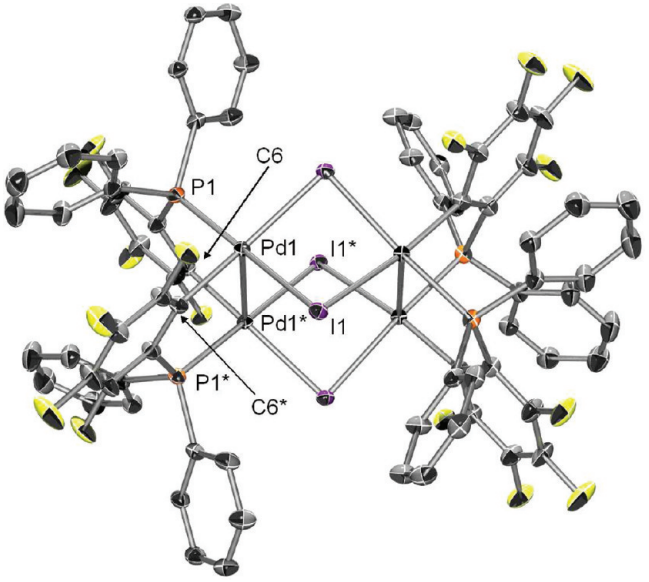

Figure 4. Molecular structure of $[Pd_4(\mu\text{-}I)_4(\mu\text{-}2\text{-}C_6F_4PPh_2)_4]$ (**13**). Ellipsoids show 50% probability levels. Hydrogen atoms and dichloromethane of crystallization have been omitted for clarity. Asterisks denote atoms generated by symmetry. Selected bond distances (Å) and angles (deg): Pd(1)···Pd(1*) 3.0841(3), Pd(1)−I(1) 2.6525(2), Pd(1*)−I(1) 2.6813(2), Pd(1)−P(1) 2.2542(6), Pd(1)−I(1)−Pd(1*) 90.907(7).

were present. The ESI-mass spectrum of **12** showed a peak at m/z 1155, corresponding to the $[M + Na]^+$ ion, confirming the dinuclear formulation. The ^{31}P NMR spectrum showed two multiplet resonances at δ −78.2 and −81.1, presumably arising from *cis*−*trans* isomers, as in the chloro and bromo analogues **5** and **8**, whose relative intensity varied between different preparations; the lower field resonance was always the more intense.

Attempts on separate occasions to obtain X-ray quality crystals of **12** gave prisms that, in one case, proved to be the tetranuclear species $[Pd_4(\mu\text{-}I)_4(\mu\text{-}2\text{-}C_6F_4PPh_2)_4]$ (**13**) (Figure 4) and in the other, $[(\kappa^2\text{-}2\text{-}C_6F_4PPh_2)Pd(\mu\text{-}I)(\mu\text{-}2\text{-}C_6F_4PPh_2)Pd(\mu\text{-}I)_2Pd(\mu\text{-}I)(\mu\text{-}2\text{-}C_6F_4PPh_2)Pd(\kappa^2\text{-}2\text{-}C_6F_4PPh_2)]$ (**14**) (Figure 5), both being formed by facile dimerization of **12**.

Selected bond distances and angles of **13** and **14** are shown in the captions to Figures 4 and 5, respectively. Complex **13** is structurally similar to the tetranuclear complexes $[Pd_4(\mu\text{-}X)_4(\mu\text{-}2\text{-}C_6H_4PPh_2)_4]$ (X = Cl, Br),[19,20] consisting of a pair of planar Pd_2I_2 units bridged by two pairs of $2\text{-}C_6F_4PPh_2$ ligands, each in a head-to-tail arrangement. The palladium atoms and, separately, the iodide ligands occupy opposite vertices of a cube. The distance between the two palladium atoms in **13** bridged by the $2\text{-}C_6F_4PPh_2$ groups [3.0841(3) Å] is similar to those reported for $[Pd_4(\mu\text{-}X)_4(\mu\text{-}2\text{-}C_6H_4PPh_2)_4]$ [X = Cl (3.09 Å), Br (3.07 Å)]; the Pd−P and Pd−C bond lengths in **13** are also comparable. The Pd−I−Pd bridges are slightly asymmetric, the Pd−I bonds *trans* to phosphorus [2.6525(2) Å] being slightly shorter than those *trans* to carbon [2.6813(2) Å]. A similar trend has been observed in the dinuclear palladium complexes $[Pd_2(\mu\text{-}I)_2(PPh_3)_2(C_6H_4\text{-}4\text{-}PPh_3)_2][OTf]_2$[36] and *anti*-$[Pd_2(\mu\text{-}I)_2(Ph)_2(PPh_3)_2]$.[37]

Complex **14** consists of four palladium atoms in a zigzag arrangement, the two symmetry-related halves of the molecule being connected by a $Pd_2(\mu\text{-}I)_2$ unit. In each half of the structure, the two metal atoms are bridged by another iodine atom and a $2\text{-}C_6F_4PPh_2$ group, the phosphorus atom of which is bound to the terminal palladium atom, Pd(1). The remaining coordination sites on Pd(1) are occupied by a chelate $\kappa^2\text{-}2\text{-}C_6F_4PPh_2$ ligand, while the coordination sphere of the inner palladium atom, Pd(2), comprises three bridging iodine atoms and the carbon atom of $\mu\text{-}2\text{-}C_6F_4PPh_2$. As expected, the coordination geometry of the palladium atoms is distorted square planar and the bite angle of the chelate $2\text{-}C_6F_4PPh_2$ ligands is ca. 69°. The separation between the metal atoms Pd(1) and Pd(2) that are bridged by $2\text{-}C_6F_4PPh_2$ and iodide [3.0305(9) Å] is significantly smaller than the corresponding separations in **13** [3.0841(3) Å]. This closer approach is also manifested in the Pd(1)−I(1)−Pd(2) angle [69.76(2)°], which is significantly smaller than the Pd(2)−I(2)−Pd(2*) angle [93.25(2)°]. The Pd−P bond lengths in the chelate $2\text{-}C_6F_4PPh_2$ groups [2.2647(19) Å] are significantly shorter than those in the bridging $2\text{-}C_6F_4PPh_2$ groups [2.326(2) Å], while the reverse trend is apparent for the Pd−C bond lengths [2.059(8) and 1.997(7) Å, respectively]. The $Pd_2(\mu\text{-}I)_2$ unit in **14** shows similar asymmetry to that in **13**, the Pd−I bonds *trans* to phosphorus [2.6808(7) Å] being slightly shorter than those *trans* to carbon [2.7009(7) Å], and

dx.doi.org/10.1021/om200179v |*Organometallics* 2011, 30, 3749–3762

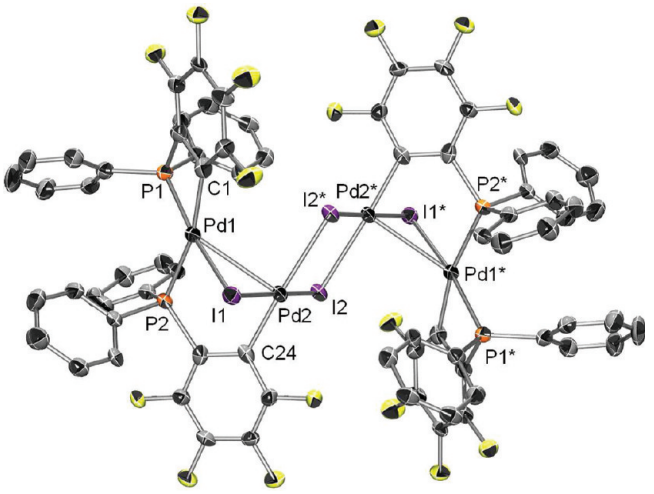

Figure 5. Molecular structure of $[(\kappa^2\text{-}2\text{-}C_6F_4PPh_2)Pd(\mu\text{-}I)(\mu\text{-}2\text{-}C_6F_4PPh_2)Pd(\mu\text{-}I)_2Pd(\mu\text{-}I)(\mu\text{-}2\text{-}C_6F_4PPh_2)Pd(\kappa^2\text{-}2\text{-}C_6F_4PPh_2)]$ (**14**). Hydrogen atoms and dichloromethane of crystallization have been omitted for clarity. Ellipsoids show 50% probability levels. Asterisks denote atoms generated by symmetry. Selected bond distances (Å) and angles (deg): Pd(1)···Pd(2) 3.0305(8), Pd(1)−I(1) 2.6808(7), I(2)−Pd(2) 2.6074(7), Pd(1)−C(6) 2.059(8), Pd(1)−P(1) 2.2647(19), Pd(1)−P(2) 2.326(2), Pd(2)−C(24) 1.997(7), Pd(2)−I(1) 2.6176(7), Pd(2)−I(2*) 2.7009(7), Pd(2)−I(1)−Pd(1) 69.76(2).

Scheme 6

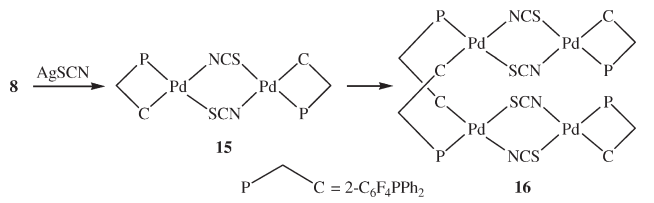

both being significantly longer than those *trans* to iodide [2.6176(7), 2.6074(7) Å].

When a solution of **12** was set aside over several days, the high-field resonance in the ^{31}P NMR spectrum diminished in intensity and a peak at δ 21.8 assignable to bridging 2-$C_6F_4PPh_2$ appeared, but this process did not go to completion. The final spectrum may correspond to a mixture of **13** and **14**, which could not be separated.

c. Thiocyanate Ions (Scheme 6). Reaction of **8** with silver thiocyanate gave an 80% yield of the corresponding thiocyanato-bridged complex $[Pd_2(\mu\text{-}SCN)_2(\kappa^2\text{-}2\text{-}C_6F_4PPh_2)_2]$ (**15**), which showed a single resonance at δ −78.2 in its ^{31}P NMR spectrum and a peak at m/z 1019 in its ESI-mass spectrum, corresponding to the $[M + Na]^+$ ion. The IR spectrum showed a strong ν(C≡N) band at 2142 cm^{-1}, typical of bridging thiocyanate,[38] cf. 2120 cm^{-1} for the structurally characterized complex $[P(CH_2Ph)Ph_3]_2[Pd_2(\mu\text{-}SCN)_2(2,4,6\text{-}C_6H_2F_3)_4]$.[39] The molecular structure of **15**, together with selected bond lengths and angles, is shown in Figure 6; it is similar to that of the bromo analogue **8** described above. Two planar-coordinated palladium atoms end-bridged by a pair of thiocyanate ligands in a head-to-tail arrangement are each coordinated by a chelate 2-$C_6F_4PPh_2$ ligand in which the phosphorus atoms are *trans* to the sulfur atoms of the SCN bridges. The Pd−P

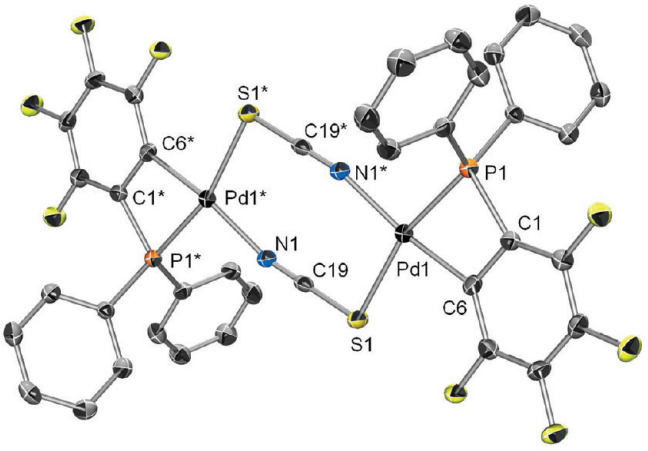

Figure 6. Molecular structure of $[Pd_2(\mu\text{-}SCN)_2(\kappa^2\text{-}2\text{-}C_6F_4PPh_2)_2]$ (**15**). Ellipsoids show 50% probability levels. Hydrogen atoms have been omitted for clarity. Asterisks denote atoms generated by symmetry. Selected bond lengths (Å) and angles (deg): Pd(1)−P(1) 2.2594(8), Pd(1)−C(6) 2.015(3), Pd(1)−S(1) 2.3980(8), Pd(1)−N(1*) 2.060(2), N(1*)−Pd(1)−S(1) 94.24(7), S(1)−Pd(1)−C(6) 95.14(9), C(6)−Pd(1)−P(1) 69.84(9), P(1)−Pd(1)−N(1*) 100.86(7), Pd(1)−N(1*)−C(19*) 165.6(2), Pd(1)−S(1)−C(19) 100.36(10), S(1)−C(19)−N(1) 178.8(3).

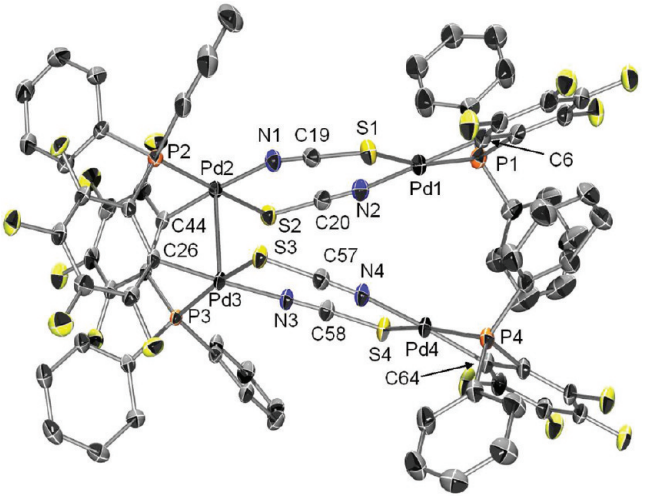

Figure 7. Molecular structure of $[Pd_4(\mu\text{-}SCN)_4(\kappa^2\text{-}2\text{-}C_6F_4PPh_2)_2(\mu\text{-}2\text{-}C_6F_4PPh_2)_2]$ (**16**). Ellipsoids show 50% probability levels. Hydrogen atoms and dichloromethane of crystallization have been omitted for clarity. Selected bond distances (Å) and angles (deg): Pd(2)···Pd(3) 2.9532(3), Pd(1)−C(6) 2.015(3), Pd(4)−C(64) 1.999(3), Pd(2)−C(44) 1.999(3), Pd(3)−C(26) 2.010(3), P(1)−Pd(1) 2.2576(9), P(2)−Pd(2) 2.2736(8), P(3)−Pd(3) 2.2893(8), P(4)−Pd(4) 2.2734(8), Pd(1)−S(1) 2.3852(9), Pd(2)−S(2) 2.3959(9), Pd(3)−S(3) 2.4008(8), Pd(4)−S(4) 2.3908(8), Pd(1)−N(2) 2.066(3), Pd(2)−N(1) 2.051(3), Pd(4)−N(4) 2.078(3), Pd(3)−N(3) 2.028(3), P(1)−Pd(1)−C(6) 69.84(10), P(4)−Pd(4)−C(64) 92.28(10).

and Pd−C bond lengths in **15** are comparable with, but slightly greater than, those in **8**. The thiocyanate ligands are almost perfectly linear, the S(1)−C(19)−N(1) angle being 178.8(3)°. As expected, the Pd−N−C unit is almost linear, the Pd(1)−N(1*)−C(19*) angle being 165.6(2)°, whereas the Pd−S−C unit is bent [Pd(1)−S(1)−C(19) 100.36(10)°]. The Pd−P, Pd−C, and

dx.doi.org/10.1021/om200179v |*Organometallics* 2011, 30, 3749–3762

Scheme 7

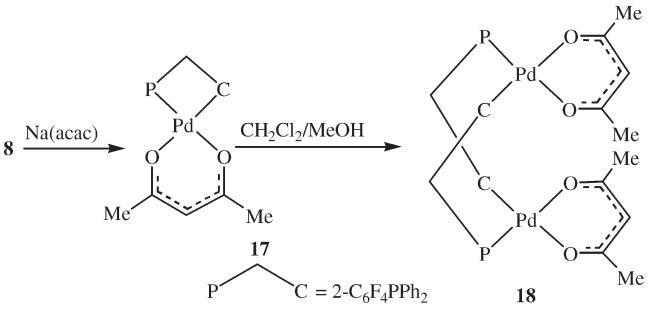

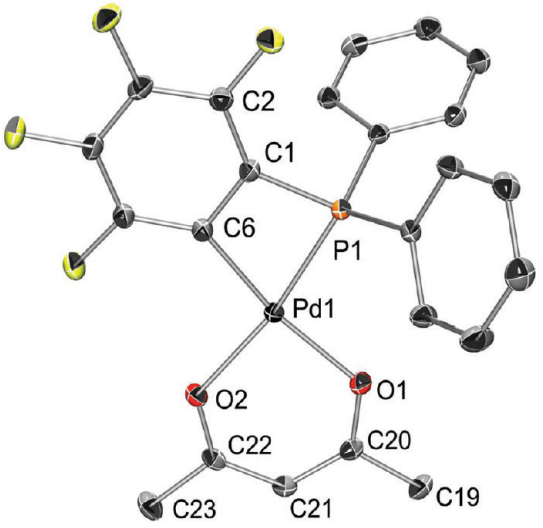

Figure 8. Molecular structure of $[Pd(acac)(\kappa^2\text{-}2\text{-}C_6F_4PPh_2)]$ (**17**). Ellipsoids show 50% probability levels. Hydrogen atoms have been omitted for clarity. Selected bond lengths (Å) and angles (deg): Pd(1)−P(1) 2.2285(3), Pd(1)−C(6) 2.0124(12), Pd(1)−O(1) 2.0603(9), Pd(1)−O(2) 2.0594(9), O(1)−C(20) 1.2723(15), O(2)−C(22) 1.2768(15), P(1)−Pd(1)−C(6) 70.13(4), O(1)−Pd(1)−O(2) 92.06(4).

Pd−S bond lengths are unexceptional, as is the bite angle of the chelate 2-$C_6F_4PPh_2$ group.

When heated to 60 °C for 3−5 h, a toluene solution of **15** became pale yellow; from the solution a pale yellow solid was isolated. Its ^{31}P NMR spectrum showed a pair of equally intense singlets at δ +19.5 and −78.0, indicative of bridging and chelating 2-$C_6F_4PPh_2$ groups, respectively. The ESI-mass spectrum showed a peak at m/z 1991 and the IR spectrum contained strong ν(C≡N) bands at 2143 and 2157 cm^{-1}, consistent with bridging thiocyanato ligands. These data suggest that the isolated solid is $[Pd_4(\mu\text{-}SCN)_4(\kappa^2\text{-}2\text{-}C_6F_4PPh_2)_2(\mu\text{-}2\text{-}C_6F_4PPh_2)_2]$ (**16**), which was confirmed by X-ray crystallography. The molecular structure of **16** is shown in Figure 7, together with selected bond lengths and angles.

The structure of **16** consists of two stacked molecules of **15** in which the 2-$C_6F_4PPh_2$ ligands at one end have undergone ring-opening so as to bridge the palladium atoms of the other molecule. The metal−ligand bond lengths in **16** are comparable to those in **15**. Attempts to open the remaining chelate rings of **16** to give $[Pd_4(\mu\text{-}SCN)_4(\mu\text{-}2\text{-}C_6F_4PPh_2)_4]$ by further heating were unsuccessful.

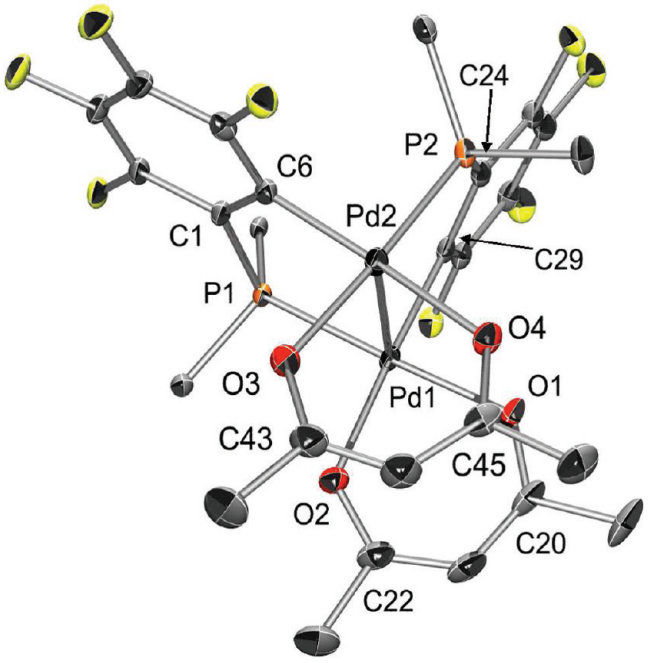

Figure 9. Molecular structure of $[Pd_2(acac)_2(\mu\text{-}2\text{-}C_6F_4PPh_2)_2]$ (**18**). Ellipsoids show 20% probability levels. Hydrogen atoms have been omitted for clarity, and only the *ipso* carbons of the PPh_2 groups are shown. Selected bond distances (Å) and angles (deg): Pd(1)···Pd(2) 2.9640(3), Pd(1)−P(1) 2.2290(7), Pd(2)−P(2) 2.2422(7), Pd(1)−C(29) 2.001(3), Pd(2)−C(6) 2.001(3), Pd(1)−O(1) 2.0666(19), Pd(1)−O(2) 2.060(2), Pd(2)−O(3) 2.050(2), Pd(2)−O(4) 2.047(2), O(1)−Pd(1)−O(2) 90.44(9), O(4)−Pd(2)−O(3) 91.33(9).

d. Acetylacetonate Ion (Scheme 7). A monomeric acetylacetonato (acac) derivative of palladium, $[Pd(acac)(\kappa^2\text{-}2\text{-}C_6F_4PPh_2)]$ (**17**), was obtained from the reaction of **8** with Na(acac) as a pale yellow solid in 84% yield. The ^{31}P NMR spectrum showed a single peak at δ −71.9, and the parent ion peak at m/z 538 was observed in the EI-mass spectrum. The ^{1}H NMR spectrum showed the expected aromatic multiplets in addition to three singlet resonances at δ 2.01, 2.12, and 5.45 in a ratio of 3:3:1 due to the two methyl and methine protons, respectively, of the acac ligand. The IR spectrum contained strong bands at 1517 and 1579 cm^{-1}, arising from the CO/CC stretching modes of bidentate acac, cf. 1524 and 1569 cm^{-1} in $[Pd(acac)_2]$.[40] In the structure of **17**, shown in Figure 8, the palladium atom is coordinated by a chelate 2-$C_6F_4PPh_2$ ligand forming one four-membered ring with a bite angle of ca. 70° and the two oxygen atoms of the acac group to complete the square-planar geometry. The Pd−O bond lengths of 2.0603(9) and 2.0594(9) Å are slightly larger than those in $[Pd(acac)_2]$ [1.9815(10), 1.9837(10) Å],[41] consistent with the greater *trans*-influence of P- and C-donor ligands.

When a solution of **17** in dichloromethane/methanol was set aside at room temperature for 2 d, or heated at 60 °C for 4 h, the resonance at δ −71.9 was replaced cleanly by a singlet at δ 24.5, indicating that the four-membered ring had been opened. No change occurred under similar conditions in the absence of methanol. The yellow solid isolated from dichloromethane/methanol was shown by X-ray crystallography to be the dinuclear complex $[Pd_2(acac)_2(\mu\text{-}2\text{-}C_6F_4PPh_2)_2]$ (**18**); the molecular structure is shown in Figure 9 together with selected bond lengths and angles. A second crystal modification of compound

dx.doi.org/10.1021/om200179v |*Organometallics* 2011, 30, 3749–3762

Scheme 8

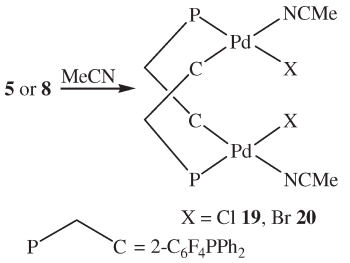

Scheme 9

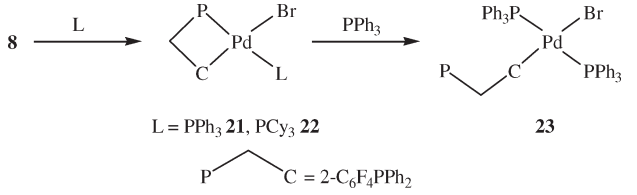

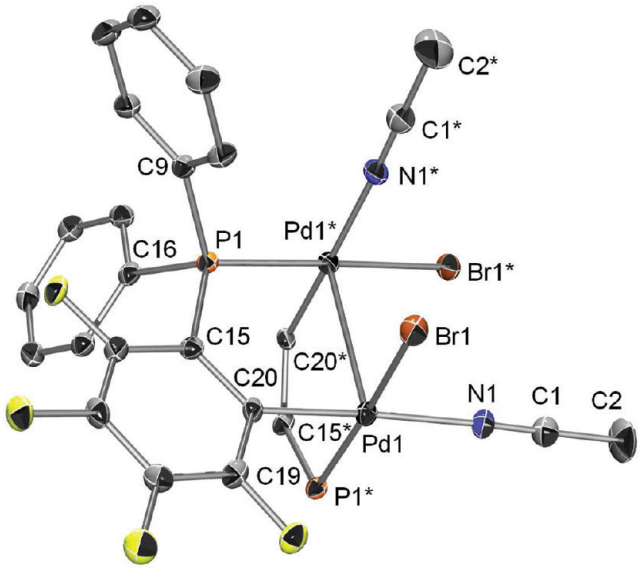

Figure 10. Molecular structure of $[Pd_2Br_2(NCMe)_2(\mu\text{-}2\text{-}C_6F_4PPh_2)_2]$ (**20**). Hydrogen atoms and solvent molecules have been omitted for clarity. Only the bridging atoms of one of the $C_6F_4PPh_2$ ligands are shown. Selected bond distances (Å) and angles (deg): Pd(1)···Pd(1*) 3.0184(3), Pd(1)−P(1*) 2.2653(6), Pd(1)−C(20) 2.001(2), Pd(1)−N(1) 2.072(2), Pd(1)−Br(1) 2.4976(3), N(1)−C(1) 1.144(3), Pd(1)−N(1)−C(1) 177.6(2), N(1)−Pd(1)−P(1*) 93.96(6), N(1)−Pd(1)−Br(1) 91.07(6), C(20)−Pd(1)−P(1*) 88.05(7), C(20)−Pd(1)−Br(1) 86.69(6), P(1*)−Pd(1)−Br(1) 174.125(18), C(20)−Pd(1)−N(1) 174.92(9).

18 (a solvate comprising one hexane molecule per formula unit of **18**) was obtained by layering the solution of **18** with *n*-hexane. Except for the fact that in the latter the center of the Pd···Pd separation of **18** is located on a 2-fold axis and the asymmetric unit therefore comprises 0.5 **18**·C_6H_{14}, the molecular architectures of the dinuclear palladium complex are very similar in these two structures, so only the first is discussed as a representative example. The structure consists of a pair of palladium atoms, each of which is coordinated in a planar array by a chelate O-bound acac group together with a phosphorus atom and a carbon atom from a pair of bridging 2-$C_6F_4PPh_2$ groups. The Pd···Pd separation [2.9640(3) Å] is similar to that in **16** [2.9532(3) Å]. The metal−ligand bond lengths in **17** and **18** are generally similar, the Pd−C distances in the latter being ca. 0.01 Å shorter than in the former. The three ^{1}H resonances characteristic of the acac methine and methyl groups in **18** are each shifted upfield by ca. 0.3 ppm relative to those of **17**, possibly reflecting a ring-current effect of the delocalized π-electrons in the acac rings that lie over each other in the structure. The IR spectrum of **18** contains two strong CC/CO bands in similar positions to those of **17**.

e. Acetonitrile (Scheme 8). On standing overnight, acetonitrile solutions of $[Pd_2(\mu\text{-}X)_2(\kappa^2\text{-}2\text{-}C_6F_4PPh_2)_2]$ [X = Cl (**5**), Br (**8**)] deposited yellow solids of formula $[Pd_2X_2(MeCN)_2(\mu\text{-}2\text{-}C_6F_4PPh_2)_2]$ [X = Cl (**19**), Br (**20**)], which each showed a ^{31}P NMR singlet at δ ca. 27, suggestive of the presence of bridging 2-$C_6F_4PPh_2$. The presence of coordinated acetonitrile was indicated by the presence in the ^{1}H NMR spectra in C_6D_6 of a singlet at δ ca. 0.6 due to CH_3 and, in the IR spectra, of a strong ν(C≡N) band at 2300 cm^{-1}.[42] The ESI-mass spectra showed peaks due to $[M]^+$ and $[M - \text{halide}]^+$.

Complex **19** crystallized from hot acetonitrile with one molecule of water (monoclinic, space group *C*2/*c*). Two solvates of **20** were obtained: a mono(acetonitrile) solvate (monoclinic, space group $P2_1/n$) and a benzene solvate (monoclinic, space group *C*2/*c*). The X-ray structure of the last is shown in Figure 10, together with selected metrical data. It consists of a pair of palladium atoms bridged by two, mutually *cis*, 2-$C_6F_4PPh_2$ ligands in a head-to-tail arrangement; a halide ligand *trans* to phosphorus and a nitrogen-bound acetonitrile ligand *trans* to carbon complete the essentially planar coordination sphere about each palladium atom. The Pd···Pd separations are similar to those of the other Pd-μ-$C_6F_4PPh_2$ complexes discussed previously. The Pd−halide distances [2.3649(3) Å (**19**); 2.4889(5), 2.4976(3) Å (**20**), acetonitrile and benzene solvates, respectively] are in the expected ranges for halide *trans* to a tertiary phosphine coordinated to Pd(II), cf., 2.351(1), 2.358(2) Å in $[PdCl_2(dppp)]$[43] and 2.4744(9), 2.4767(9) Å in $[PdBr_2(dppp)]$ [dppp = 1,3-bis(diphenylphosphino)propane].[44]

f. Tertiary Phosphines (Scheme 9). The halide bridges in $[Pd_2(\mu\text{-}Br)_2(\kappa^2\text{-}2\text{-}C_6F_4PPh_2)_2]$ (**8**) were rapidly cleaved by PPh_3 or PCy_3 to give the mononuclear complexes *cis*- and *trans*-$[PdBr(\kappa^2\text{-}2\text{-}C_6F_4PPh_2)L]$ [L = PPh_3 (**21**), PCy_3 (**22**)], isolated as pale yellow solids. The ^{31}P NMR spectra of **21** and **22** each showed a pair of resonances at δ ca. −80 and +30, assignable to a chelate 2-$C_6F_4PPh_2$ group and coordinated PR_3 ligand, respectively. Each resonance was split into a doublet of doublets of ca. 490 Hz, typical of *trans* P−P coupling. The resonance at δ ca. 30 in **21** was further split by ca. 8 Hz due to coupling with the *ortho*-fluorine of the $C_6F_4PPh_2$ group. Low-intensity peaks at δ ca. −75 and +17 (**21**) and ca. δ −73 and +26 (**22**) corresponding to the *cis* isomers were also observed. The ratio of *cis*/*trans* isomers for **21** and **22** varied between preparations, but was typically about 1:9 in both cases; the *trans* isomer always predominated.

The structure of *trans*-$[PdBr(\kappa^2\text{-}2\text{-}C_6F_4PPh_2)(PPh_3)]$ (*trans*-**21**) has been confirmed by X-ray diffraction and is shown in Figure 11, together with selected bond distances and angles. It

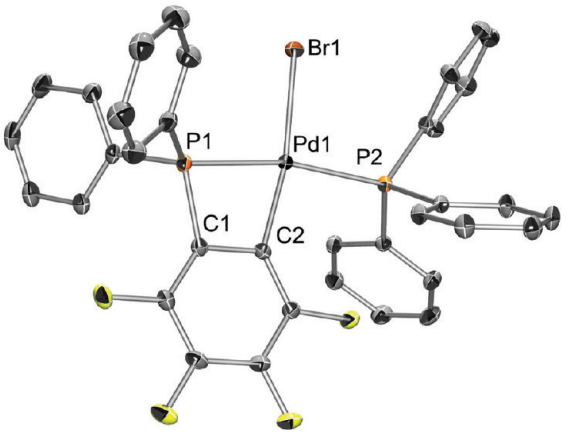

Figure 11. Molecular structure of *trans*-[PdBr(κ^2-2-$C_6F_4PPh_2$)-(PPh_3)] (*trans*-**21**). Ellipsoids show 30% probability levels. Hydrogen atoms have been omitted for clarity. Selected bond lengths (Å) and angles (deg): Pd(1)−P(1) 2.3178(5), Pd(1)−P(2) 2.3355(5), Pd-(1)−Br(1) 2.4723(2), Pd(1)−C(2) 2.0440(17), P(1)−Pd(1)−C(2) 69.32(5).

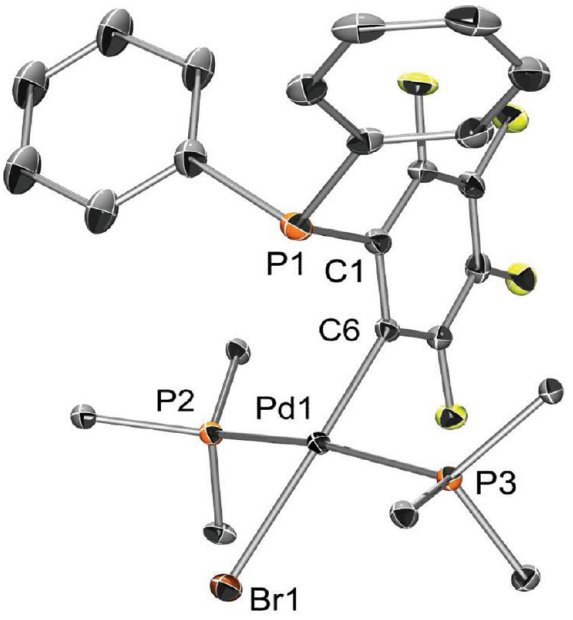

Figure 12. Molecular structure of *trans*-[PdBr(κC-2-$C_6F_4PPh_2$)-(PPh_3)$_2$] (**23**). Hydrogen atoms have been omitted for clarity, and only the *ipso* carbons of the PPh_3 ligands are shown. Selected bond distances (Å) and angles (deg): Pd(1)−C(6) 2.0296(19), Pd(1)−P(2) 2.3349(5), Pd(1)−P(3) 2.3416(5), Pd(1)−Br(1) 2.5033(2), C(6)−Pd(1)−P(2) 90.41(6), C(6)−Pd(1)−P(3) 92.72(6), P(2)−Pd(1)−P(3) 168.553(19), C(6)−Pd(1)−Br(1) 177.18(6).

consists of a palladium atom coordinated to an *ortho*-metalated 2-$C_6F_4PPh_2$ group forming a four-membered chelate ring. One PPh_3 ligand *trans* to the phosphorus atom of the metalated group and one bromide complete the coordination about the metal center. The geometry about the palladium atom is distorted from square planar as a result of the narrow bite angle (ca. 69°) of the chelate 2-$C_6F_4PPh_2$ ligand. The Pd−Br distance is about 0.11 and 0.03 Å, respectively, shorter than those in the structurally similar compounds *trans*-[PdBr(κ^2-2-$C_6H_4PPh_2$)(L)] [L = PPh_2(2-BrC_6H_4),[20] $C_5H_5FeC_5H_4PPh_2$[45]], consistent with the lower *trans* influence of a fluoroaryl group relative to that of its aryl counterpart.[46]

The chelate ring in [PdBr(κ^2-2-$C_6F_4PPh_2$)(PPh_3)] (**21**) was opened by the addition of a stoichiometric amount of PPh_3 to give *trans*-[PdBr(κC-2-$C_6F_4PPh_2$)(PPh_3)$_2$] (**23**), in which the PPh_2 group of the fluoroaryl ligand is not bound to the metal atom. The ^{31}P NMR spectrum of **23** showed two resonances in a 2:1 ratio at δ 20.7 and −3.7, the chemical shifts being typical of, respectively, tertiary arylphosphines coordinated to Pd(II) and free tertiary arylphosphines. The molecular structure of **23** has been confirmed by X-ray crystallography and is shown in Figure 12, together with selected metrical parameters.

In the structure of **23**, the square-planar-coordinated palladium atom is bound to two phosphorus atoms of mutually *trans* PPh_3 ligands, one bromide, and a C-bonded 2-$C_6F_4PPh_2$ group. The phosphorus atom of the 2-$C_6F_4PPh_2$ group is oriented above the palladium atom, and the large Pd(1)−P(1) separation (ca. 3.4 Å) indicates that there is little or no Pd−P interaction. The metal−ligand bond lengths are similar to those in *trans*-**21**.

DISCUSSION

The reaction of 2-$Me_3SnC_6F_4PPh_2$ in a 1:1 mol ratio at room temperature with [PdX_2(cod)] gives the halide-bridged dimers [$Pd_2(\mu$-X)$_2$(κ^2-2-$C_6F_4PPh_2$)$_2$] [X = Cl (**5**), Br (**8**)] in good yields; this method is probably more convenient and provides a purer product than ligand scrambling of the bis(chelate) complex *trans*-[Pd(κ^2-2-$C_6F_4PPh_2$)$_2$] with [PdX_2(NCMe)$_2$].[24] We have shown previously that 2-$Me_3SnC_6F_4PPh_2$ is also a convenient alternative to 2-$LiC_6F_4PPh_2$ in the preparation of the digold(I) complex [$Au_2(\mu$-2-$C_6F_4PPh_2$)$_2$].[23] Following the pioneering work of Eaborn, Pidcock, et al.,[47−50] (aryl)trimethyltin reagents have been used extensively for the selective transfer, under mild conditions, of one or two aryl groups to platinum(II),[51−57] but in the case of palladium(II) the reaction is usually successful only when, as in our case, the aryl groups bear a donor center.[58−60]

The [$Pd_2(\mu$-X)$_2$(κ^2-2-$C_6F_4PPh_2$)$_2$] complexes are not thermodynamically stable; they rearrange in solution, either at room temperature or on heating, to give complexes containing μ-2-$C_6F_4PPh_2$. The rearrangement is probably initiated by one-ended dissociation of the Pd−P bond, driven by the relief of strain in the four-membered ring. The facile, stepwise displacement of the phosphorus atoms of [Pt(κ^2-2-$C_6H_4PPh_2$)$_2$] by P-donors (L) to give [Pt(κC-2-$C_6H_4PPh_2$)$_2$L$_2$][61] and the reaction of [PdBr(κ^2-2-$C_6F_4PPh_2$)(PPh_3)] (**21**) with PPh_3 to give *trans*-[PdBr(κC-2-$C_6F_4PPh_2$)(PPh_3)] (**23**) described here provide models for the initial dissociation step. The rearrangements are promoted by polar or coordinating solvents, such as methanol and acetonitrile, which may stabilize the necessary vacant sites on the metal atoms. However, as shown by the behavior of the iodo and thiocyanato complexes, **12** and **15**, respectively, not all the available chelate groups necessarily undergo rearrangement, for reasons that are not clear.

Although complex **21** has a 2-$C_6H_4PPh_2$ analogue (Scheme 1), there are no known κ^2-2-$C_6H_4PPh_2$ analogues of the [Pd_2X_2(κ^2-2-$C_6F_4PPh_2$)$_2$] complexes; palladaphosphaarene and palladaphosphacyclobutene complexes of this type are known only when there are bulky substituents, such as 2-tolyl[62] or *tert*-butyl,[63] in the cyclopalladated ring. The stabilizing effect on metal−aryl binding of electronegative fluorine in place of hydrogen in the aromatic ring is evident from published surveys of transition metal−C_6F_5 complexes;[64,65] complete replacement of hydrogen by fluorine

dx.doi.org/10.1021/om200179v |*Organometallics* 2011, 30, 3749–3762

also serves to slow down, if not completely inhibit, the transformation from chelate to bridging coordination of the 2-$C_6H_4PPh_2$ group. Two other observations point to the same conclusion: (1) the chelate rings of *trans*-[M(κ^2-2-$C_6F_4PPh_2$)$_2$] (M = Ni, Pd, Pt)[24] do not undergo $\kappa^2 \rightarrow \mu$ rearrangement when the complexes are heated, whereas *cis*-[Pt(κ^2-2-$C_6H_4PPh_2$)$_2$] dimerizes on heating to give [Pt$_2$(κ^2-2-$C_6H_4PPh_2$)$_2$(μ-2-$C_6H_4PPh_2$)$_2$],[22] and (2) 2-$Me_3SnC_6H_4PPh_2$ reacts with [PdX_2(cod)] at room temperature to give the tetramers [Pd$_4$(μ-X)$_4$(μ-2-$C_6H_4PPh_2$)$_4$] as the only isolable product.[66]

CONCLUSIONS

We have prepared and characterized structurally a series of *ortho*-palladated complexes containing the carbanion 2-$C_6F_4PPh_2$ acting as a four-membered chelate ligand, e.g., [Pd$_2$(μ-Br)$_2$(κ^2-*P*,*C*-2-$C_6F_4PPh_2$)$_2$], most of which have not been isolated so far with the corresponding carbanion 2-$C_6H_4PPh_2$. The κ^2-2-$C_6F_4PPh_2$ complexes usually rearrange at room temperature to give complexes of the same composition that contain the carbanion as a bridging ligand, μ-2-$C_6F_4PPh_2$, via solvent- or ligand-assisted opening of the chelate ring. Some of the analogous μ-2-$C_6H_4PPh_2$ compounds are known. We believe that a facile chelate to bridging transformation of this type has not been demonstrated previously in solutions of *ortho*-metalated triarylphosphine complexes. Two compounds have been discovered in which only half the available chelate 2-$C_6F_4PPh_2$ groups have undergone ring-opening, together with one compound in which the carbanion is bound to palladium through the σ-carbon atom only.

EXPERIMENTAL SECTION

General Procedures. Reactions were performed under an atmosphere of dry argon with the use of standard Schlenk techniques. All glassware was oven-dried overnight. Acetone was dried over molecular sieves and acetonitrile was refluxed over calcium hydride and distilled under nitrogen; all other solvents were dried by the use of a standard column drying system. The compounds 2-$BrC_6F_4PPh_2$,[67] [PdX_2(cod)] (X = Cl, Br),[68] and Na(acac)[69] were prepared by the appropriate literature methods; all other reagents were commercially available and used as received.

Physical Measurements. Elemental analyses were performed by the Microanalytical Unit of the Research School of Chemistry at The Australian National University (ANU). ^{1}H (300 MHz), ^{13}C (75 MHz), and ^{31}P (121 MHz) NMR spectra were recorded on a Bruker Avance 300 spectrometer in C_6D_6, unless otherwise stated. Coupling constants (*J*) are given in hertz, and chemical shifts (δ) are given in ppm, internally referenced to residual solvent signals (^{1}H, ^{13}C) or external 85% H_3PO_4 (^{31}P). Mass spectra were recorded on a Bruker Apex 3 FTICR or a Micromass Platform mass spectrometer (RMIT). Accurate mass determinations were carried out on a Waters ESI-TOF Premier XE instrument (ANU). Raman spectra were obtained on a Perkin-Elmer Raman Station 400 as solid samples in glass capillary tubes. Infrared spectra (4000−400 cm^{-1}) were obtained on a Perkin-Elmer Spectrum 2000 FT-IR spectrometer as KBr disks.

X-ray Crystallography. Crystals suitable for single-crystal X-ray diffraction were obtained by layering a CH_2Cl_2 or benzene solution of the complex with hexane or methanol, or by slow evaporation from acetonitrile. Using a drop of Paratone (inert oil), crystals were mounted on a glass capillary and transferred to a stream of cold nitrogen. The reflection data were collected on a Nonius Kappa CCD diffractometer equipped with a 95 mm camera and graphite-monochromated Mo Kα radiation (λ = 0.71073 Å), in φ- and ω-scan modes.

Data were measured by use of COLLECT.[70] The intensities of reflections were extracted and the data were reduced by use of the computer programs Denzo, SORTAV, and Scalepack.[71,72] The crystal structures of **7**−**11**, **13**−**20**, and **23** were solved by direct methods with the use of SHELXS-97[73] or by the Patterson method in SHELXS-97. Structure refinement on F^2 was carried out by a full-matrix least-squares procedure with the use of SHELXL-97.[74] The structure of **21** was solved and refined on F^2 with use of the programs SIR92[75] and CRYSTALS,[76] respectively. Refinement of the modulated structure of **8**·CH_2Cl_2 was performed on *F* using the program RAELS2006[77] with a weighting scheme that included an uncorrelated 3% error in F_{obs} in addition to the counting statistics error for F_{obs}. Because of weak intensity of the higher order satellite reflections, it was decided to use a constrained refinement model, and 870 independent variables were used to describe 249 non-hydrogen atom positions and their atomic displacement parameters. Hydrogen atoms were reinserted in geometrically sensible positions after each refinement cycle and given atom displacement parameters determined by the parameters describing the atoms to which they are attached. The complex has pseudo 2/*m* local symmetry, so the constrained models used refinable local orthonormal coordinates relative to refinable local orthonormal axial systems to force chemically equivalent ring systems to have an equal local planar geometry that was refinable while not constraining the connectivity of these rings. Atom displacement parameters for these rings and attached F or H atoms were refined using *T*, *TL*, or *TLX* parametrizations.[78] Each disordered phenyl ring was described by a six-variable *T* model, each ordered phenyl ring was described by a 12-variable *TL* model centered on the P atom to which it was attached, and each C_6F_4 fragment was described using a 15-variable *TLX* model. CCDC reference numbers 799192−799209 refer to the crystal structures reported in this paper.

Syntheses. *2-$Me_3SnC_6F_4PPh_2$ (**7**).* A solution of 2-$BrC_6F_4PPh_2$ (6.6 g, 16 mmol) in ether (100 mL) was cooled to −78 °C and treated slowly with a solution of ^{n}BuLi (1.6 M in hexanes, 10.0 mL, 16 mmol). After stirring the mixture for 30 min, Me_3SnCl (1.0 M in hexanes, 16.0 mL, 16 mmol) was added dropwise and the solution was stirred at −78 °C for 2 h. After being allowed to warm to room temperature, the suspension was hydrolyzed and the ether layer was separated. The aqueous phase was extracted with ether (3 × 50 mL), and the combined organic phases were dried ($MgSO_4$). After filtration, the solvent was removed and the gummy solid was recrystallized from hot methanol to give white crystals of the title compound (6.9 g, 87%).

Mp: 77−79 °C. ^{1}H NMR ($CDCl_3$): δ 0.48 (t, *J* = 1.6 Hz with ^{117}Sn/^{119}Sn satellites, *J* = 54.9, 57.8 Hz, 9H, $SnMe_3$), 7.2−7.4 (m, 10H, aromatics). ^{13}C NMR ($CDCl_3$): δ −3.9 (dd, *J* = 4.5, 13.3 Hz with ^{117}Sn/^{119}Sn satellites, *J* = 361, 381 Hz) together with 128.5 (d, *J* = 6.4 Hz), 128.8 (s), 132.4 (dd, *J* = 1.8, 18.9 Hz), 134.6 (dd, *J* = 2.2, 9.2 Hz) due to the PPh_2 carbons and low-intensity peaks at δ 125.5 (m), 140.7 (m), 141.5 (m), 148.7 (m), 150.1 (m), 150.7 (m) due to the C_6F_4 carbons. ^{31}P NMR ($CDCl_3$): δ −0.2 (ddd, *J* = 1.6, 2.9, 22.8 Hz with unresolved ^{117}Sn/^{119}Sn satellites, *J* = 29.4 Hz). ESI-MS (*m*/*z*): 499 [M + H]$^+$. Anal. Calcd for $C_{21}H_{19}F_4PSn$: C 50.75, H 3.85, F 15.29. Found: C 51.04, H 3.96, F 15.32.

*[Pd$_2$(μ-Cl)$_2$(κ^2-2-$C_6F_4PPh_2$)$_2$] (**5**).* A mixture of 2-$Me_3SnC_6F_4PPh_2$ (500 mg, 1.0 mmol) and [$PdCl_2$(cod)] (287 mg, 1.0 mmol) was dissolved in CH_2Cl_2 (15 mL) to give a yellow solution, and after 2 h, the solvent and volatile byproducts were removed *in vacuo*. The residue was dissolved in CH_2Cl_2, hexane was added, and the solution was evaporated under reduced pressure until a bright yellow solid precipitated. This was isolated by filtration, washed with hexane, and dried *in vacuo* to give **5** (400 mg, 84%). The ratio of *trans*:*cis* isomers estimated from the ^{31}P NMR spectrum was ca. 1.5:1, but varied between preparations.

^{1}H NMR: δ 6.7−7.5 (m, 20H, aromatics). ^{31}P NMR: δ −76.8 (br s), −77.5 (br s). ESI-MS (m/z): 970.8255; calcd 970.8257 $[M + Na]^+$. Anal. Calcd for $C_{36}H_{20}Cl_2F_8P_2Pd_2$: C 45.51, H 2.12, Cl 7.46, F 16.00. Found: C 45.41, H 2.43, Cl 7.33, F 15.90.

[Pd$_2$(μ-Br)$_2$(κ^2-2-C$_6$F$_4$PPh$_2$)$_2$] (**8**). This compound was made similarly to **5** from 2-Me$_3$SnC$_6$F$_4$PPh$_2$ (500 mg, 1.0 mmol) and [PdBr$_2$(cod)] (376 mg, 1.0 mmol) in CH_2Cl_2 (15 mL) and was obtained as a dark yellow solid (460 mg, 88%). The *trans*:*cis* ratio was ca. 3:1, but varied between preparations.

^{1}H NMR: δ 6.7−7.5 (m, 20H, aromatics). ^{31}P NMR: δ −76.5 (br s), −77.9 (br s). ESI-MS (m/z): 1058.7267; calcd 1058.7246 $[M + Na]^+$. Anal. Calcd for $C_{36}H_{20}Br_2F_8P_2Pd_2$: C 41.61, H 1.94, Br 15.38, F 14.63. Found: C 41.75, H 2.13, Br 15.30, F 15.14.

[Pd$_2$(μ-O$_2$CCH$_3$)$_2$(κ^2-2-C$_6$F$_4$PPh$_2$)$_2$] (**9**). To a solution of **8** (100 mg, 0.1 mmol) in CH_2Cl_2 (15 mL) was added AgOAc (30 mg, 0.3 mmol), and the mixture was stirred for 30 min in the dark, during which time the color of the suspension faded to pale yellow. The insoluble silver salts were removed by filtration, and the volume of the filtrate was reduced by half under reduced pressure. Addition of hexane precipitated a pale yellow solid, which was isolated by filtration, washed with hexane, and dried to give **9** (75 mg, 78%).

^{1}H NMR: δ 2.26 (s, 6H, Me), 6.6−7.2 and 7.9−8.2 (m, 20H, aromatics). ^{31}P NMR: δ −73.9 (br s). ESI-MS (m/z): 1019 $[M + Na]^+$. IR (ν, cm^{-1}): 1421 and 1567 (COO str.). Anal. Calcd for $C_{40}H_{26}F_8O_4P_2Pd_2$: C 48.17, H 2.63, F 15.24. Found: C 48.39, H 2.96, F 14.50.

[Pd$_2$(μ-O$_2$CPh)$_2$(κ^2-2-C$_6$F$_4$PPh$_2$)$_2$] (**10**). This compound was made analogously to **9** above from **8** (100 mg, 0.1 mmol) and AgOBz (65 mg, 0.3 mmol) in CH_2Cl_2 (15 mL). The yield of **10** was 80 mg (74%).

^{1}H NMR: δ 6.7−8.7 (m, 30H, aromatics). ^{31}P NMR: δ −74.3 (br s). ESI-MS (m/z): 1145 $[M + Na]^+$. IR (ν, cm^{-1}): 1396 and 1596 (COO str.). Anal. Calcd for $C_{50}H_{30}F_8O_4P_2Pd_2$: C 53.55, H 2.70, F 13.55. Found: C 53.20, H 2.87, F 13.09.

[Pd$_2$(μ-I)$_2$(κ^2-2-C$_6$F$_4$PPh$_2$)$_2$] (**12**). A solution of **9** (100 mg, 0.1 mmol) in dichloromethane (10 mL) was treated with a solution of NaI (45 mg, 0.3 mmol) in methanol (10 mL). After stirring the mixture for 15 min, the solvents were evaporated under reduced pressure. The residue was extracted with dichloromethane, the solution was filtered through Celite, and the filtrate was evaporated to dryness to give a dark brown solid, which consisted mainly of a mixture of *trans* and *cis* isomers (2:1) of **12** (91 mg, 80%). In some preparations, variable amounts of unidentified impurities were also present.

^{1}H NMR: δ 6.2−8.6 (m, 20H, aromatics). ^{31}P NMR: δ −78.2 (br s), −81.1 (br s). ESI-MS (m/z): 1154.6993; calcd 1154.6969 $[M + Na]^+$. Anal. Calcd for $C_{36}H_{20}F_8I_2P_2Pd_2$: C 38.16, H 1.78, F 13.41, I 22.40. Found: C 38.31, H 1.74, F 13.46, I 22.35.

[Pd$_2$(μ-SCN)$_2$(κ^2-2-C$_6$F$_4$PPh$_2$)$_2$] (**15**). To a dark yellow solution of **8** (100 mg, 0.1 mmol) in CH_2Cl_2 (15 mL) was added AgSCN (50 mg, 0.3 mmol). The solution became turbid, and after stirring for 15 min in the dark, the suspension was filtered through Celite to give a pale yellow solution. Hexane was added and the volume was partially evaporated under reduced pressure to precipitate the product as a pale yellow solid, which was isolated by filtration, washed with hexane, and dried *in vacuo* (81 mg, 84%).

^{31}P NMR: δ −78.2 (br s). ESI-MS (m/z): 1019 $[M + Na]^+$. IR (ν, cm^{-1}): 2142 (C≡N str.). Anal. Calcd for $C_{38}H_{20}F_8N_2P_2Pd_2S_2$: C 45.85, H 2.03, N 2.81, F 15.27, S 6.44. Found: C 45.73, H 2.31, N 2.85, F 15.48, S 6.25.

[Pd$_4$(μ-SCN)$_4$(κ^2-2-C$_6$F$_4$PPh$_2$)$_2$(μ-2-C$_6$F$_4$PPh$_2$)$_2$] (**16**). A toluene solution (15 mL) of **15** (100 mg, 0.1 mmol) was heated to 60 °C for 3−5 h, during which time the solution became almost colorless. Addition of hexane precipitated **16**, which was separated by filtration, washed with hexane, and dried *in vacuo* (80 mg, 80%).

^{1}H NMR: δ 6.7−8.2 (m, 40H, aromatics). ^{31}P NMR: δ 19.5 (br s), −78.0 (br s). ESI-MS (m/z): 1991 $[M]^+$. IR (ν, cm^{-1}): 2143 and 2157 (C≡N str.). Anal. Calcd for $C_{76}H_{40}F_{16}N_4P_4Pd_4S_4$: C 45.55, H 2.03, N 2.81. Found: C 45.47, H 2.39, N 2.77.

[Pd(acac)(κ^2-2-C$_6$F$_4$PPh$_2$)] (**17**). To a dark yellow solution of **8** (100 mg, 0.1 mmol) in CH_2Cl_2 (15 mL) was added Na(acac) (50 mg, 0.3 mmol). The solution became turbid, and, after stirring for 30 min, the suspension was filtered through Celite to give a pale yellow solution. Hexane was added and the solution was evaporated under reduced pressure to precipitate the product as a pale yellow solid, which was isolated by filtration, washed with hexane, and dried *in vacuo* (81 mg, 84%).

^{1}H NMR ($CDCl_3$): δ 2.01 (s, 3H, Me), 2.12 (s, 3H, Me), 5.45 (s, 1H, CH of acac), 7.4−7.9 (m, 10H, aromatics). ^{31}P NMR (C_6D_6): δ −71.9 (br s). EI-MS (m/z): 538 $[M]^+$. IR (ν, cm^{-1}): 1517 (CO str.) and 1579 (CC str.). Anal. Calcd for $C_{23}H_{17}F_4O_2PPd$: C 51.28, H 3.18, F 14.11. Found: C 51.11, H 3.30, F 13.80.

[Pd$_2$(μ-acac)$_2$(μ-2-C$_6$F$_4$PPh$_2$)$_2$] (**18**). A solution of complex **17** (100 mg, 0.19 mmol) in a 1:1 mixture of dichloromethane and methanol (20 mL) was stirred at room temperature for 2 d. The solvents were evaporated under reduced pressure, and the residue was extracted with dichloromethane. Filtration through Celite and evaporation of the solvent gave **18** (154 mg, 75%).

^{1}H NMR ($CDCl_3$): δ 1.61 (s, 6H, Me), 1.74 (s, 6H, Me), 5.07 (s, 2H, CH of acac), 7.3−8.1 (m, 20H, aromatics). ^{31}P NMR: δ 24.5 (br s). IR (ν, cm^{-1}): 1517 (CO str.) and 1579 (CC str.). Anal. Calcd for $C_{46}H_{34}F_8O_4P_2Pd_2$: C 51.28, H 3.18, F 14.11. Found: C 50.99, H 3.06, F 14.14.

[Pd$_2$Cl$_2$(NCMe)$_2$(μ-2-C$_6$F$_4$PPh$_2$)$_2$] (**19**). A yellow solution of **5** (100 mg, 0.1 mmol) in MeCN (10 mL) was stirred overnight. The bright yellow solid that precipitated was isolated by filtration, washed with MeCN, and dried *in vacuo* (90 mg, 83%).

^{1}H NMR: δ 0.59 (s, 6H, MeCN), 6.7−8.1 (m, 20H, aromatics). ^{31}P NMR: δ 27.8 (br s). ESI-MS (m/z): 997 $[M - Cl]^+$. IR (ν, cm^{-1}): 2294 cm^{-1} (C≡N str.). Anal. Calcd for $C_{40}H_{26}Cl_2F_8N_2P_2Pd_2$: C 46.54, H 2.54, N 2.71, Cl 6.87, F 14.72. Found: C 45.92, H 2.58, N 2.43, Cl 6.58, F 14.47.

[Pd$_2$Br$_2$(NCMe)$_2$(μ-2-C$_6$F$_4$PPh$_2$)$_2$] (**20**). The title compound was made from **8** (100 mg, 0.1 mmol) by the same procedure as described above (95 mg, 88%).

^{1}H NMR: δ 0.58 (s, 6H, MeCN), 6.7−8.1 (m, 20H, aromatics). ^{31}P NMR: δ 27.5 (br s). ESI-MS (m/z): 1121 $[M]^+$. IR (ν, cm^{-1}): 2299 cm^{-1} (C≡N str.). Anal. Calcd for $C_{40}H_{26}Br_2F_8N_2P_2Pd_2$: C 42.85, H 2.34, N 2.50, Br 14.25, F 13.56. Found: C 42.25, H 2.31, N 2.02, Br 14.26, F 13.52.

[PdBr(κ^2-2-C$_6$F$_4$PPh$_2$)(PPh$_3$)] (**21**). A solution of **8** (180 mg, 0.17 mmol) in CH_2Cl_2 (5 mL) was treated with PPh_3 (91 mg, 0.34 mmol) at room temperature. Hexane was immediately added, and the volume of the yellow solution was reduced *in vacuo*. The precipitated pale yellow solid was isolated by filtration, washed with hexane, and dried *in vacuo* (264 mg, 97%). The *trans*:*cis* ratio was generally ca. 9:1, but varied between preparations.

^{1}H NMR ($CDCl_3$): δ 5.3 (s, 2H, CH_2Cl_2), 7.1−8.2 (m, 25H, aromatics). ^{31}P NMR: δ −84.0 (d, J = 490 Hz), 29.3 (dd, J = 489, 8.0 Hz), −75.2 (br s), 17.1 (d, J = 14.0 Hz). ESI-MS (m/z): 783 $[M + H]^+$. Anal. Calcd for $C_{36}H_{25}BrF_4P_2Pd \cdot 0.3CH_2Cl_2$: C 54.00, H 3.20, Br 9.90, Cl 2.63, F 9.41. Found: C 54.70, H 3.03, Br 9.46, Cl 2.92, F 9.58.

[PdBr(κ^2-2-C$_6$F$_4$PPh$_2$)(PCy$_3$)] (**22**). To an orange solution of **8** (100 mg, 0.1 mmol) in CH_2Cl_2 (10 mL) was added PCy_3 (55 mg, 0.2 mmol). After 5 min, hexane was added and the solution was evaporated under reduced pressure. The very pale yellow solid that precipitated was isolated similarly to **21**. The yield was 75 mg (80%). The *trans*:*cis* ratio was ca. 9:1, but varied between preparations.

^{1}H NMR: δ 1.2−1.4, 1.5−1.9, 2.0−2.4, 2.8−3.1 (m, 33H, Cy), 7.1−7.4 and 8.2−8.5 (m, 10H, aromatics). ^{31}P NMR: δ −86.7 (d, J = 462 Hz), 37.9 (d, J = 462 Hz), −73.1 (br s), 26.7 (d, J = 14.8 Hz). Anal. Calcd for $C_{36}H_{43}BrF_4P_2Pd$: C 54.05, H 5.42, Br 9.99. Found: C 53.85, H 5.42, Br 9.83.

[PdBr(κC-2-C$_6$F$_4$PPh$_2$)(PPh$_3$)$_2$] (**23**). To a yellow solution of **21** (100 mg, 0.13 mmol) in CH_2Cl_2 (15 mL) was added PPh_3 (33.5 mg, 0.13 mmol). The solution was stirred for 30 min at room temperature. The solution was partially evaporated under reduced pressure, and hexane was added to precipitate **23** (116 mg, 87%).

^{1}H NMR: δ 6.8−8.0 (m, 40 H, aromatics). ^{31}P NMR: δ −3.7 (br s), 20.7 (s). ESI-MS (m/z): 1043 $[M - H]^+$. Anal. Calcd for $C_{54}H_{40}BrF_4P_3Pd$: C 62.12, H 3.86, Br 7.65, F 7.28. Found: C 62.54, H 3.90, Br 7.48, F 6.88.

X-ray Crystal Structure Data. *2-Me$_3$SnC$_6$F$_4$PPh$_2$* (**7**). Empirical formula $C_{21}H_{19}F_4PSn$, fw = 497.02, temperature 110(2) K, monoclinic, space group $P2_1/c$, a = 7.7721(1) Å, b = 27.0559(4) Å, c = 19.2390(3) Å, β = 95.172(1)°, V = 4029.13(10) Å^3, Z = 8, ρ_{calcd} = 1.639 Mg/m^3, crystal dimensions 0.40 × 0.32 × 0.27 mm^3, 100 829 reflections, 21 885 independent (R_{int} = 0.0651), μ = 1.386 mm^{-1}, 487 parameters, 0 restraints, R_1 = 0.0352 ($I > 2\sigma$), wR_2 (all data) = 0.0711, GOF = 1.037, largest diff. peak and hole 0.629/−0.776 e Å^{-3}.

[Pd$_2$Br$_2$(κ^2-2-C$_6$F$_4$PPh$_2$)$_2$]·CH$_2$Cl$_2$ (**8**). Empirical formula $C_{37}H_{22}Br_2Cl_2F_8P_2Pd_2$, fw = 1123.99, temperature 110(2) K, triclinic, space group $P\bar{1}$, a = 19.5851(3) Å, b = 20.3668(4) Å, c = 23.0951(4) Å, α = 104.989(1)°, β = 102.553(1)°, γ = 102.556(1)°, V = 8312.4(3) Å^3, Z = 9, ρ_{calcd} = 2.021 Mg/m^3, crystal dimensions 0.40 × 0.25 × 0.10 mm^3, 252 823 reflections, 62 527 independent (R_{int} = 0.1178), μ = 3.437 mm^{-1}, 870 parameters, 0 restraints, R_1 = 0.0490 ($I > 2\sigma$), wR_2 (all data) = 0.1259, GOF = 1.33, max./min. residual electron density: 2/−2 e Å^{-3}.

Complex **8** crystallizes as a 9-fold superstructure that can be regarded as a commensurate modulation of a Z = 1 parent structure with unit cell axes $a = 1/9(2a - 3b + c)$, $b = 1/9(4a + 3b + 2c)$, $c = 1/3(-a + c)$ and one-ninth the cell volume.

[Pd$_2$(μ-O$_2$CCH$_3$)$_2$(κ^2-2-C$_6$F$_4$PPh$_2$)$_2$]·0.5C$_6$H$_6$ (**9**). Empirical formula $C_{43}H_{29}O_4F_8P_2Pd_2$, fw = 1036.40, temperature 90(2) K, monoclinic, space group $P2_1/n$, a = 12.3560(1) Å, b = 16.7991(2) Å, c = 19.4832(2) Å, β = 105.467(1)°, V = 3897.66(7) Å^3, Z = 4, ρ_{calcd} = 1.766 Mg/m^3, crystal dimensions 0.24 × 0.18 × 0.18 mm^3, 144 509 reflections, 21 221 independent (R_{int} = 0.0649), μ = 1.087 mm^{-1}, 532 parameters, 0 restraints, R_1 = 0.0315 ($I > 2\sigma$), wR_2 (all data) = 0.0666, GOF = 1.038, max./min. residual electron density 0.675/−0.836 e Å^{-3}.

[Pd$_2$(μ-O$_2$CPh)$_2$(κ^2-2-C$_6$F$_4$PPh$_2$)$_2$]] (**10**). Empirical formula $C_{50}H_{30}F_8O_4P_2Pd_2$, fw = 1121.48, temperature 110(2) K, triclinic, space group $P\bar{1}$, a = 11.5541(2) Å, b = 12.2585(2) Å, c = 16.5603(3) Å, α = 93.640(1)°, β = 93.386(1)°, γ = 110.655(1)°, V = 2181.99(7) Å^3, Z = 2, ρ_{calcd} = 1.707 Mg/m^3, crystal dimensions 0.45 × 0.22 × 0.10 mm^3, 78 921 reflections, 20 656 independent (R_{int} = 0.0581), μ = 0.979 mm^{-1}, 595 parameters, 0 restraints, R_1 = 0.0313 ($I > 2\sigma$), wR_2 (all data) = 0.0769, GOF = 1.048, max./min. residual electron density 0.925/−1.345 e Å^{-3}.

[Pd$_2$(μ-O$_2$CCH$_3$)$_2$(μ-2-C$_6$F$_4$PPh$_2$)$_2$]·C$_6$H$_6$ (**11**). Empirical formula $C_{46}H_{32}F_8O_4P_2Pd_2$, fw = 1075.46, temperature 90(2) K, monoclinic, space group $C2/c$, a = 21.6513(3) Å, b = 9.5972(2) Å, c = 20.2274(3) Å, β = 106.178(1)°, V = 4036.65(12) Å^3, Z = 4, ρ_{calcd} = 1.770 Mg/m^3, crystal dimensions 0.24 × 0.22 × 0.16 mm^3, 72 254 reflections, 14 016 independent (R_{int} = 0.0508), μ = 1.053 mm^{-1}, 280 parameters, 0 restraints, R_1 = 0.0305 ($I > 2\sigma$), wR_2 (all data) = 0.0736, GOF = 1.053, max./min. residual electron density 1.511/−1.571 e Å^{-3}.

[Pd$_2$(μ-O$_2$CCH$_3$)$_2$(μ-2-C$_6$F$_4$PPh$_2$)$_2$] (**11**). Empirical formula $C_{40}H_{26}F_8O_4P_2Pd_2$, fw = 997.35, temperature 110(2) K, orthorhombic, space group $Pna2_1$, a = 19.7970(3) Å, b = 9.9514(1) Å, c = 18.0698(3) Å, V = 3559.89(9) Å^3, Z = 4, ρ_{calcd} = 1.861 Mg/m^3, crystal dimensions 0.12 × 0.06 × 0.03 mm^3, 52 431 reflections, 8467 independent (R_{int} = 0.0906), μ = 1.186 mm^{-1}, 505 parameters, 1 restraint, R_1 = 0.0383 ($I > 2\sigma$), wR_2 (all data) = 0.0825, GOF = 1.051, max./min. residual electron density 0.740/−0.991 e Å^{-3}.

[Pd$_4$(μ-I)$_4$(μ-2-C$_6$F$_4$PPh$_2$)$_4$]·1.68CH$_2$Cl$_2$ (**13**). Empirical formula $C_{73.68}H_{43.36}Cl_{3.36}F_{16}I_4P_4Pd_4$, fw = 2408.80, temperature 100(2) K, orthorhombic, space group *Fddd*, a = 18.7731(2) Å, b = 22.8802(3) Å, c = 35.4070(4) Å, V = 15208.5(3) Å^3, Z = 8, ρ_{calcd} = 2.104 Mg/m^3, crystal dimensions 0.22 × 0.20 × 0.18 mm^3, 65 859 reflections, 7176 independent (R_{int} = 0.0734), μ = 2.839 mm^{-1}, 247 parameters, 1 restraint, R_1 = 0.0286 ($I > 2\sigma$), wR_2 (all data) = 0.0713, GOF = 1.023, max./min. residual electron density 3.040/−1.179 e Å^{-3}.

[(κ^2-2-C$_6$F$_4$PPh$_2$)Pd(μ-I)(μ-2-C$_6$F$_4$PPh$_2$)Pd(μ-I)$_2$Pd(μ-I)(μ-2-C$_6$F$_4$-PPh$_2$)Pd(κ^2-2-C$_6$F$_4$PPh$_2$)]·2CH$_2$Cl$_2$ (**14**),. Empirical formula $C_{74}H_{44}Cl_4F_{16}I_4P_4Pd_4$, fw = 2435.97, temperature 100(2) K, triclinic, space group $P\bar{1}$, a = 10.0756(3) Å, b = 13.3568(5) Å, c = 16.5002(6) Å, α = 83.309(2)°, β = 76.136(2)°, γ = 71.196(2)°, V = 2038.94(12) Å^3, Z = 1, ρ_{calcd} = 1.984 Mg/m^3, crystal dimensions 0.07 × 0.05 × 0.03 mm^3, 35 118 reflections, 7979 independent (R_{int} = 0.0388), μ = 2.669 mm^{-1}, 493 parameters, 46 restraints, R_1 = 0.0495 ($I > 2\sigma$), wR_2 (all data) = 0.1263, GOF = 1.068, max./min. residual electron density 1.844/−1.917 e Å^{-3}.

[Pd$_2$(μ-SCN)$_2$(κ^2-2-C$_6$F$_4$PPh$_2$)$_2$] (**15**). Empirical formula $C_{38}H_{20}F_8N_2P_2Pd_2S_2$, fw = 995.42, temperature 110(2) K, monoclinic, space group $P2_1/n$, a = 8.2531(3) Å, b = 17.7696(5) Å, c = 12.3228(4) Å, β = 93.809(2)°, V = 1803.20(10) Å^3, Z = 2, ρ_{calcd} = 1.833 Mg/m^3, crystal dimensions 0.19 × 0.05 × 0.04 mm^3, 28 711 reflections, 4784 independent (R_{int} = 0.0775), μ = 1.276 mm^{-1}, 244 parameters, 0 restraints, R_1 = 0.0374 ($I > 2\sigma$), wR_2 (all data) = 0.0808, GOF = 1.053, max./min. residual electron density 1.090/−0.868 e Å^{-3}.

[Pd$_4$(μ-SCN)$_4$(κ^2-2-C$_6$F$_4$PPh$_2$)$_2$(μ-2-C$_6$F$_4$PPh$_2$)$_2$]·2.5CH$_2$Cl$_2$ (**16**). Empirical formula $C_{78.50}H_{45}Cl_5F_{16}N_4P_4Pd_4S_4$, fw = 2203.16, temperature 100(2) K, triclinic, space group $P\bar{1}$, a = 13.5687(3) Å, b = 16.0586(3) Å, c = 20.6429(5) Å, α = 91.7337(10)°, β = 97.6461(10)°, γ = 110.4889(10)°, V = 4161.64(16) Å^3, Z = 2, ρ_{calcd} = 1.758 Mg/m^3, crystal dimensions 0.35 × 0.25 × 0.20 mm^3, 92 367 reflections, 26 517 independent (R_{int} = 0.0633), μ = 1.270 mm^{-1}, 1098 parameters, 129 restraints, R_1 = 0.0454 ($I > 2\sigma$), wR_2 (all data) = 0.1189, GOF = 1.061, max./min. residual electron density 2.239/−1.486 e Å^{-3}.

[Pd(acac)(κ^2-2-C$_6$F$_4$PPh$_2$)] (**17**). Empirical formula $C_{23}H_{17}F_4O_2PPd$, fw = 538.74, temperature 110(2) K, monoclinic, space group $P2_1/n$, a = 14.5018(2) Å, b = 13.2373(2) Å, c = 22.7098(3) Å, β = 108.237(1)°, V = 4140.50(10) Å^3, Z = 8, ρ_{calcd} = 1.728 Mg/m^3, crystal dimensions 0.37 × 0.27 × 0.11 mm^3, 107 158 reflections, 22 422 independent (R_{int} = 0.0540), μ = 1.728 mm^{-1}, 559 parameters, 0 restraints, R_1 = 0.0344 ($I > 2\sigma$), wR_2 (all data) = 0.0770, GOF = 1.058, max./min. residual electron density 0.718/−0.829 e Å^{-3}.

[Pd$_2$(μ-acac)$_2$(μ-2-C$_6$F$_4$PPh$_2$)$_2$] (**18**). Empirical formula $C_{46}H_{34}F_8O_4P_2Pd_2$, fw = 1077.47, temperature 150(2) K, monoclinic, space group $P2_1/n$, a = 11.5391(2) Å, b = 29.6519(7) Å, c = 13.1661(3) Å, β = 109.696(1)°, V = 4241.30(16) Å^3, Z = 4, ρ_{calcd} = 1.687 Mg/m^3, crystal dimensions 0.19 × 0.07 × 0.06 mm^3, 62 815 reflections, 11 260 independent (R_{int} = 0.0522), μ = 1.003 mm^{-1}, 588 parameters, 74 restraints, R_1 = 0.0381 ($I > 2\sigma$), wR_2 (all data) = 0.0866, GOF = 1.051, max./min. residual electron density 0.942/−0.756 e Å^{-3}.

[Pd$_2$(μ-acac)$_2$(μ-2-C$_6$F$_4$PPh$_2$)$_2$].C$_6$H$_{14}$ (**18**). Empirical formula $C_{52}H_{48}F_8O_4P_2Pd_2$, fw = 1163.64, temperature 110(2) K, monoclinic, space group $C2/c$, a = 16.5901(3) Å, b = 25.6576(6) Å, c = 11.3881(2) Å, β = 90.314(1)°, V = 4847.41(17) Å^3, Z = 4, ρ_{calcd} = 1.594 Mg/m^3, crystal dimensions 0.17 × 0.13 × 0.12 mm^3, 47 195 reflections, 7068 independent (R_{int} = 0.0691), μ = 0.884 mm^{-1}, 319 parameters, 2 restraints, R_1 = 0.0332 ($I > 2\sigma$), wR_2 (all data) = 0.0821, GOF = 1.078, max./min. residual electron density 0.893/−0.975 e Å^{-3}.

[Pd$_2$Cl$_2$(NCMe)$_2$(μ-2-C$_6$F$_4$PPh$_2$)$_2$] (**19**). Empirical formula $C_{40}H_{26}Cl_2F_8N_2OP_2Pd_2$, fw = 1050.28, temperature 90(2) K, monoclinic, space group $C2/c$, a = 20.0714(4) Å, b = 18.9384(5) Å, c = 10.4669(2) Å,

β = 103.150(1)°, V = 3874.35(15) Å^3, Z = 4, ρ_{calcd} = 1.801 Mg/m^3, crystal dimensions 0.28 × 0.15 × 0.06 mm^3, 65 109 reflections, 13 502 independent (R_{int} = 0.0562), μ = 1.224 mm^{-1}, 270 parameters, 12 restraints, R_1 = 0.0339 ($I > 2\sigma$), wR_2 (all data) = 0.0756, GOF = 1.053, max./min. residual electron density 1.696/−1.100 e Å^{-3}.

[Pd$_2$Br$_2$(NCMe)$_2$(μ-2-C$_6$F$_4$PPh$_2$)$_2$]·C$_6$H$_6$ (**20**),. Empirical formula $C_{46}H_{32}Br_2F_8N_2P_2Pd_2$, fw = 1199.30, temperature 100(2) K, monoclinic, space group $C2/c$, a = 19.2331(4) Å, b = 17.0626(4) Å, c = 14.8104(3) Å, β = 118.144(1)°, V = 4285.62(16) Å^3, Z = 4, ρ_{calcd} = 1.859 Mg/m^3, crystal dimensions 0.12 × 0.08 × 0.06 mm^3, 58 115 reflections, 7433 independent (R_{int} = 0.0850), μ = 2.850 mm^{-1}, 282 parameters, 0 restraints, R_1 = 0.0372 ($I > 2\sigma$), wR_2 (all data) = 0.0900, GOF = 1.031, max./min. residual electron density 1.091/−1.350 e Å^{-3}.

[Pd$_2$Br$_2$(NCMe)$_2$(μ-2-C$_6$F$_4$PPh$_2$)$_2$]·CH$_3$CN (**20**). Empirical formula $C_{42}H_{29}Br_2F_8N_3P_2Pd_2$, fw = 1162.24, temperature 110(2) K, monoclinic, space group $P2_1/n$, a = 13.0981(4) Å, b = 16.0475(6) Å, c = 20.4163(8) Å, β = 101.936(2)°, V = 4198.6(3) Å^3, Z = 4, ρ_{calcd} = 1.839 Mg/m^3, crystal dimensions 0.33 × 0.16 × 0.07 mm^3, 36 031 reflections, 12 198 independent (R_{int} = 0.0781), μ = 2.907 mm^{-1}, 541 parameters, 14 restraints, R_1 = 0.0467 ($I > 2\sigma$), wR_2 (all data) = 0.0853, GOF = 1.042, max./min. residual electron density 0.848/−1.062 e Å^{-3}.

trans-[PdBr(κ^2-2-C$_6$F$_4$PPh$_2$)(PPh$_3$)] (**21**). Empirical formula $C_{36}H_{25}BrF_4P_2Pd$, fw = 781.84, temperature 200 K, monoclinic, space group $P2_1/n$, a = 9.9090(1) Å, b = 14.4677(1) Å, c = 21.3719(2) Å, β = 94.5475(6)°, V = 3054.24(5) Å^3, Z = 4, ρ_{calcd} = 1.700 Mg/m^3, crystal dimensions 0.22 × 0.19 × 0.03 mm^3, 78 537 reflections, 8939 independent (R_{int} = 0.039), μ = 2.07 mm^{-1}, 397 parameters, 0 restraints, max./min. residual electron density 1.5/−2.92 e Å^{-3}.

trans-[PdBr(κC-2-C$_6$F$_4$PPh$_2$)(PPh$_3$)$_2$] (**23**). Empirical formula $C_{54}H_{40}BrF_4P_3Pd$, fw = 1044.08, temperature 110(2) K, orthorhombic, space group *Pbcn*, a = 34.8898(6) Å, b = 12.6979(2) Å, c = 20.4723(4) Å, V = 9069.8(3) Å^3, Z = 8, ρ_{calcd} = 1.529 Mg/m^3, crystal dimensions 0.20 × 0.14 × 0.08 mm^3, 110 769 reflections, 15 726 independent (R_{int} = 0.0704), μ = 1.450 mm^{-1}, 580 parameters, 37 restraints, R_1 = 0.0401 ($I > 2\sigma$), wR_2 (all data) = 0.0789, GOF = 1.019, max./min. residual electron density 0.654/−0.941 e Å^{-3}.

AUTHOR INFORMATION

Corresponding Author

*E-mail: suresh.bhargava@rmit.edu.au.

ACKNOWLEDGMENT

J.W. thanks the Deutscher Akademischer Austauschdienst (DAAD) for the award of a Postdoctoral Fellowship.

REFERENCES

(1) Cope, A. C.; Siekman, R. W. *J. Am. Chem. Soc.* **1965**, *87*, 3272–3273.

(2) Cope, A. C.; Friedrich, E. C. *J. Am. Chem. Soc.* **1968**, *90*, 909–913.

(3) Omae, I. *Organometallic Intramolecular Coordination Compounds*; Elsevier: Amsterdam, 1986.

(4) Newkome, G. R.; Puckett, W. E.; Gupta, V. K.; Kiefer, G. E. *Chem. Rev.* **1986**, *86*, 451–489.

(5) Ryabov, A. D. *Chem. Rev.* **1990**, *90*, 403–424.

(6) Canty, A. J. In *Comprehensive Organometallic Chemistry II*; Abel, E. W; Stone, F. G. A.; Wilkinson, G.; Puddephatt, R. J., Eds.; Pergamon: Oxford, 1995; Vol. 9, p 225.

(7) Spencer, J.; Pfeffer, M. *Adv. Met. Org. Chem.* **1998**, *6*, 103–144.

(8) Albrecht, M.; van Koten, G. *Angew. Chem., Int. Ed.* **2001**, *40*, 3750–3781.

(9) van der Boom, M. E.; Milstein, D. *Chem. Rev.* **2003**, *103*, 1759–1792.

(10) Bedford, R. B. *Chem. Commun.* **2003**, 1787–1796.

(11) Bedford, R. B.; Cazin, C. S. J.; Holder, D. *Coord. Chem. Rev.* **2004**, *248*, 2283–2321.

(12) Omae, I. *Coord. Chem. Rev.* **2004**, *248*, 995–1023.

(13) Beletskaya, I. P.; Cheprakov, A. V. *J. Organomet. Chem.* **2004**, *689*, 4055–4082.

(14) Dupont, J.; Consorti, C. S.; Spencer, J. *Chem. Rev.* **2005**, *105*, 2527–2572.

(15) Jain, V. K.; Jain, L. *Coord. Chem. Rev.* **2005**, *249*, 3075–3197.

(16) Elsevier, C. J.; Eberhard, M. R. In *Comprehensive Organometallic Chemistry III*; Mingos, D. M. P.; Crabtree, R. H.; Canty, A. J., Eds.; Elsevier: Oxford, 2007; Vol. 8, p 269.

(17) Bennett, M. A.; Contel, M.; Hockless, D. C. R.; Welling, L. L. *Chem. Commun.* **1998**, 2401–2402.

(18) Bennett, M. A.; Contel, M.; Hockless, D. C. R.; Welling, L. L.; Willis, A. C. *Inorg. Chem.* **2002**, *41*, 844–855.

(19) Aarif, A. M.; Estevan, F.; García-Bernabé, A.; Lahuerta, P.; Sanaú, M.; Ubeda, M. A. *Inorg. Chem.* **1997**, *36*, 6472–6475.

(20) Estevan, F.; García-Bernabé, A.; Lahuerta, P.; Sanaú, M.; Ubeda, M. A.; Ramírez de Arellano, M. C. *Inorg. Chem.* **2000**, *39*, 5964–5969.

(21) Bennett, M. A.; Berry, D. E.; Bhargava, S. K.; Ditzel, E. J.; Robertson, G. B.; Willis, A. C. *J. Chem. Soc., Chem. Commun.* **1987**, 1613–1615.

(22) Bennett, M. A.; Bhargava, S. K.; Messelhäuser, J.; Privér, S. H.; Welling, L. L.; Willis, A. C. *Dalton Trans.* **2007**, 3158–3169.

(23) Bennett, M. A.; Bhargava, S. K.; Mirzadeh, N.; Privér, S. H.; Wagler, J.; Willis, A. C. *Dalton Trans.* **2009**, 7537–7551.

(24) Bennett, M. A.; Bhargava, S. K.; Keniry, M. A.; Privér, S. H.; Simmonds, P. M.; Wagler, J.; Willis, A. C. *Organometallics* **2008**, *27*, 5361–5370.

(25) Nagashima, M.; Fujii, H.; Kimura, M. *Bull. Chem. Soc. Jpn.* **1973**, *46*, 3708–3711.

(26) Csákvári, É.; Shishkov, I. F.; Rozsondai, B.; Hargittai, I. *J. Mol. Struct.* **1990**, *239*, 291–303.

(27) Karipides, A.; Forman, C.; Thomas, R. H. P.; Reed, A. T. *Inorg. Chem.* **1974**, *13*, 811–815.

(28) Lin, T.-P.; Gualco, P.; Ladeira, S.; Amgoune, A.; Bourissou, D.; Gabbaí, F. P. *C. R. Chim.* **2010**, *13*, 1168–1172.

(29) Mohr, F.; Privér, S. H.; Bhargava, S. K.; Bennett, M. A. *Coord. Chem. Rev.* **2006**, *250*, 1851–1888.

(30) Koshevoy, I. O.; Lahuerta, P.; Sanaú, M.; Ubeda, M. A.; Doménech, A. *Dalton Trans.* **2006**, 5536–5541.

(31) Garrou, P. E. *Chem. Rev.* **1981**, *81*, 229–266.

(32) Nakamoto, K. *Infrared and Raman Spectra of Inorganic and Coordination Compounds, Applications in Coordination, Organometallic, and Bioinorganic Chemistry, Part B*, 6th ed.; Wiley-Interscience, 2009; p 64.

(33) Bercaw, J. E.; Durrell, A. C.; Gray, H. B.; Green, J. C.; Hazari, N.; Labinger, J. A.; Winkler, J. R. *Inorg. Chem.* **2010**, *49*, 1801–1810.

(34) Powers, D. C.; Ritter, T. *Nat. Chem.* **2009**, *1*, 302–309.

(35) Umakoshi, K.; Sasaki, Y. *Adv. Inorg. Chem.* **1994**, *40*, 187–239, and references therein.

(36) Lang, H.; Taher, D.; Walfort, B.; Pritzkow, H. *J. Organomet. Chem.* **2006**, *691*, 3834–3845.

(37) Marshall, W. J.; Young, R. J., Jr; Grushin, V. V. *Organometallics* **2001**, *20*, 523–533.

(38) Ref 32, p 125.

(39) López, G.; Garcia, G.; Santana, M. D.; Sánchez, G.; Ruiz, J.; Hermoso, J. A.; Vegas, A.; Martínez-Ripoll, M. *J. Chem. Soc., Dalton Trans.* **1990**, 1621–1626.

(40) Ref 32, p 96.

(41) Hamid, M.; Zeller, M.; Hunter, A. D.; Mazhar, M.; Tahir, A. A. *Acta Crystallogr., Sect. E* **2005**, *61*, 2181–2183.

(42) Ref 32, p 117.

(43) Steffen, W. L.; Palenik, G. J. *Inorg. Chem.* **1976**, *15*, 2432–2439.

(44) Vila, J. M.; Ortigueira, J. M.; López, M.; Fernández, J. J.; Fernández, A. *Acta Crystallogr., Sect. C* **1999**, *55*, 1646–1647.

(45) Bennett, M. A.; Bhargava, S. K.; Bond, A. M.; Burgar, I. M.; Guo, S.-X.; Kar, G.; Privér, S. H.; Wagler, J.; Willis, A. C.; Torriero, A. A. J. *Dalton Trans.* **2010**, *39*, 9079–9090.
(46) Bennett, M. A.; Bhargava, S. K.; Privér, S. H.; Willis, A. C. *Eur. J. Inorg. Chem.* **2008**, 3467–3481.
(47) Eaborn, C.; Odell, K. J.; Pidcock, A. *J. Chem. Soc., Dalton Trans.* **1978**, 357–368.
(48) Eaborn, C.; Odell, K. J.; Pidcock, A. *J. Chem. Soc., Dalton Trans.* **1978**, 1288–1294.
(49) Eaborn, C.; Odell, K. J.; Pidcock, A. *J. Chem. Soc., Dalton Trans.* **1979**, 758–760.
(50) Eaborn, C.; Kundu, K.; Pidcock, A. *J. Chem. Soc., Dalton Trans.* **1981**, 933–938.
(51) Müller, W. D.; Brune, H. A. *Chem. Ber.* **1986**, *119*, 759–761.
(52) Stapp, B.; Schmidtberg, G.; Brune, H. A. *Z. Naturforsch., Sect. B* **1986**, *41*, 514–518.
(53) Weisemann, C.; Schmidtberg, G.; Brune, H. A. *J. Organomet. Chem.* **1989**, *365*, 403, and related papers by Brune, H. A., et al. in *J. Organomet. Chem.*
(54) Deacon, G. B.; Gatehouse, B. M.; Nelson-Reed, K. T. *J. Organomet. Chem.* **1989**, *359*, 267–283.
(55) Rakowsky, M. H.; Woolcock, J. C.; Wright, L. L.; Green, D. B.; Rettig, M. F.; Wing, R. M. *Organometallics* **1987**, *6*, 1211–1218.
(56) Chantson, J. T.; Lotz, S.; Ichharam, V. *New J. Chem.* **2003**, *27*, 1735–1740.
(57) Lu, W.; Vicic, D. A.; Barton, J. K. *Inorg. Chem.* **2005**, *44*, 7970–7980.
(58) Suggs, J. W.; Lee, K. S. *J. Organomet. Chem.* **1986**, *299*, 297–309.
(59) Motoyama, Y.; Makihara, N.; Mikami, Y.; Aoki, K.; Nishiyama, H. *Chem. Lett.* **1997**, 951–952.
(60) Cera, M.; Cerrada, E.; Laguna, M.; Mata, J. A.; Teruel, H. *Organometallics* **2002**, *21*, 121–126.
(61) Bennett, M. A.; Bhargava, S. K.; Ke, M.; Willis, A. C. *J. Chem. Soc., Dalton Trans.* **2000**, 3537–3545.
(62) Christmann, U.; Pantazis, D. A.; Benet-Buchholz, J.; McGrady, J. E.; Maseras, F.; Vilar, R. *J. Am. Chem. Soc.* **2006**, *128*, 6376–6390.
(63) Yan, X.; Xi, C. *Organometallics* **2008**, *27*, 152–154.
(64) Usón, R.; Forniés, J. *Adv. Organomet. Chem.* **1988**, *28*, 219–297.
(65) García-Monforte, M. A.; Alonso, P. J.; Forniés, J.; Menjón, B. *Dalton Trans.* **2007**, 3347–3359.
(66) Bennett, M. A.; Bhargava, S. K.; Kar, G. Unpublished results.
(67) Eller, P. G.; Meek, D. W. *J. Organomet. Chem.* **1970**, *22*, 631–636.
(68) Drew, D.; Doyle, J. R. *Inorg. Synth.* **1972**, *13*, 47–55.
(69) Charles, R. G. *Org. Synth.* **1959**, *39*, 61–62.
(70) COLLECT Software. Nonius BV: Delft, The Netherlands, 1997−2001.
(71) Otwinowsky, Z.; Minor, W. *Methods Enzymol.* **1997**, *276*, 307–326.
(72) Blessing, R. H. *Acta Crystallogr., Sect. A* **1995**, *51*, 33–38.
(73) Sheldrick, G. M. *SHELXS-97, Program for the Solution of Crystal Structures*; University of Göttingen: Göttingen, Germany, 1997; *WINGX* version: release 97-2.
(74) Sheldrick, G. M. *SHELXL-97, Program for the Refinement of Crystal Structures*, University of Göttingen: Göttingen, Germany, 1997: *WINGX* version: release 97-2; See also: Sheldrick, G. M. *Acta Crystallogr., Sect. A* **2008**, *64*, 112–122.
(75) Altomare, A.; Cascarano, G.; Giocovazzo, C.; Guagliardi, A.; Burla, M. C.; Polidori, G.; Camalli, M. *J. Appl. Crystallogr.* **1994**, *27*, 435–436.
(76) Betteridge, P. W.; Carruthers, J. R.; Cooper, R. I.; Prout, K.; Watkin, D. J. *J. Appl. Crystallogr.* **2003**, *36*, 1487.
(77) Rae, A. D. *Acta Crystallogr., Sect. A* **1975**, *31*, 560−570, 570–574.
(78) Rae, A. D. *RAELS06*, A Comprehensive Constrained Least Squares Refinement Program; Australian National University, 2006.